Copyright Warning & Restrictions

The copyright law of the United States (Title 17, United States Code) governs the making of photocopies or other reproductions of copyrighted material.

Under certain conditions specified in the law, libraries and archives are authorized to furnish a photocopy or other reproduction. One of these specified conditions is that the photocopy or reproduction is not to be "used for any purpose other than private study, scholarship, or research." If a, user makes a request for, or later uses, a photocopy or reproduction for purposes in excess of "fair use" that user may be liable for copyright infringement,

This institution reserves the right to refuse to accept a copying order if, in its judgment, fulfillment of the order would involve violation of copyright law.

Please Note: The author retains the copyright while the New Jersey Institute of Technology reserves the right to distribute this thesis or dissertation

Printing note: If you do not wish to print this page, then select "Pages from: first page # to: last page #" on the print dialog screen

ABSTRACT

LOW PRESSURE CHEMICAL VAPOR DEPOSITION OF SILICON DIOXIDE AND PHOSPHOSILICATE GLASS THIN FILMS

by

Vijayalakshmi Venkatesan

Silicon dioxide thin films were synthesized on silicon and quartz wafers using Ditertiarybutylsilane(DTBS) and oxygen as precursors. Trimethylphosphite (TMP) was injected to obtain phosphosilicate glass. The films were processed at different temperatures between 700°C and 850°C at a constant pressure, and at different flow ratios of the precursors. The films deposited were uniform, amorphous and the composition of the films varied with deposition temperature and precursor flow ratios. The deposition rate increased with increasing temperature and with increasing TMP flow rate. The stresses were very low tensile in the case of undoped silicon dioxide film and tended towards being less tensile with increasing deposition temperature. The refractive index increased with increasing deposition temperature. The higher refractive index was probably because the films were rich in carbon. A less transparent film at higher temperatures also suggested presence of carbon at higher temperatures. In the case of the binary silicate glass, the stresses tended to be progressively compressive with increasing phosphorus content. The density and refractive index increased with increasing phosphorus content. Both undoped and doped oxides showed almost 99% optical transmission at a deposition temperature of 700°C. The undoped and the binary oxides showed best properties, especially optical properties, at 700°C.

LOW PRESSURE CHEMICAL VAPOR DEPOSITION OF SILICON DIOXIDE AND PHOSPHOSILICATE GLASS THIN FILMS

by
Vijayalakshmi Venkatesan

A Thesis
Submitted to the faculty of
New Jersey Institute of Technology
in Partial Fulfillment of the Requirements for the Degree of
Master of science in Engineering Science

Interdisciplinary Program in Materials Science and Engineering

October 1996

APPROVAL PAGE

LOW PRESSURE CHEMICAL VAPOR DEPOSITION OF SILICON DIOXIDE AND PHOSPHOSILICATE GLASS THIN FILMS

Vijayalakshmi Venkatesan

Thesis and Abstract Approved
by the Examining Committee

Dr. Roland A. Levy, Thesis Advisor — Date
Distinguished Professor of Physics, NJIT

Dr. Lev N. Krasnoperov — Date
Associate Professor of Chemical Engineering,
Chemistry and Environmental Sciences, NJIT

Dr. Kenneth R. Farmer — Date
Assistant Professor of Physics, NJIT

New Jersey Institute of Technology, Newark, New Jersey

BIOGRAPHICAL SKETCH

Author: Vijayalakshmi Venkatesan

Degree: Master of Science

Date: October 1996

Undergraduate and Graduate Education:

- Master of Science in Engineering Science
  New Jersey Institute of Technology
  Newark, NJ, 1996

- Bachelor of Technology (B Tech) in Metallurgical Engineering
  Indian Institute of Technology (IIT)
  Madras, India 1995

Major: Materials Science and Engineering

Professional Experience

• Research Assistant	CVD laboratory, NJIT	1995-1996
• Teaching Assistant	Department of Physics	1995-1996

This thesis is dedicated to

my parents

ACKNOWLEDGEMENT

I would like to express my sincere gratitude to my advisor, Professor Roland A Levy for his guidance, inspiration, and support throughout this research.

Special thanks to Dr. Kenneth R. Farmer and Lev N. Krasnaperov for serving as members of the thesis review committee.

I would like to thank Jan Opyrchal and Vitaly Sigal, for their help and guidance.

I would like to thank my late friend Manish Narayan for his suggestions and constant encouragement that he provided throughout the course of study at NJIT. I would also like to thank the other CVD lab members including Romiana Petrova, Mahalingam Bhaskaran, Chenna Ravindranath, Kiran V Chatty, and Krit Aryusook for their timely help and valuable suggestions. Thanks to Dr. P.K. Swain for useful suggestions.

Special thanks to my brother Pattabi Venkatesan for having been a constant source of encouragement throughout this work and always.

TABLE OF CONTENTS

TABLE OF CONTENTS
(Continued)

TABLE OF CONTENTS
(Continued)

LIST OF TABLES

LIST OF FIGURES

CHAPTER 1

INTRODUCTION

1.1 General

In the manufacture of electronic components, especially solid state devices, a wide variety of physical and chemical processes are employed. Many of these processing steps serve the single function of forming a thin layer of a given material on a suitable substrate. This layer may play an active or passive role in the operation of the component, or alternatively , it may be employed only for processing purposes and may not be present in the complete device.

Materials already in use as deposited thin films for electronic devices exhibit a tremendous range of physical phenomena. They may be superconductors, conductors, semiconductors or insulators composed of elements, compounds, or mixtures. Some can be deposited by any of the several methods; others can be handled only by a single technique.

Because of the importance of these thin film materials, the electronic industry has invested heavily in the development of new deposition technology. Chemical vapor deposition (CVD) is one of the most versatile of the deposition techniques employed in the electronics industry. In CVD, a gaseous chemical compound , or a mixture of compounds, reacts at a heated surface to form non-volatile coating on that surface. By

suitable choice of chemical reagents, it is possible to deposit an extraordinary variety of film materials on a wide range of substrates, often at rate higher than obtainable by other deposition methods such as vacuum evaporation, or sputtering. Until recently, most CVD operations were relatively simple and could be readily optimized experimentally by changing the reaction, the activation method or deposition variables until a satisfactory deposit was achieved. It is still possible and , indeed, in some cases it is the most efficient way to proceed. However, many of the CVD processes are becoming increasingly complicated with many more variables which could make the empirical method very cumbersome.

CVD is a very versatile and dynamic technology which is constantly expanding and improving as witnessed by the recent developments in Metal Organic CVD, plasma CVD, laser CVD and many others. As the technology is expanding, so is the scope of its applications. This expansion is the direct result of a large research effort carried out by many workers in the industry, the universities and government laboratories. Two major areas of application of CVD have rapidly developed, namely in the semiconductor industry and in the so-called metallurgical coating industry. CVD applications can be classified by product functions such as electrical, opto-electrical, optical, mechanical and chemical. CVD applications can also be classified by product form such as coatings, powders, fibers, monoliths and composites.

With CVD , it is almost possible to produce any metal and non-metallic element. This technology is now an essential factor in many optical and opto-electronic

applications. An integrated-optic biosensor could monitor the concentration of liquid pollutants on the surface of a planar substrate comprising single-mode channel waveguides [50]. A silica based Mach Zehnder interferometer structure on silicon could be used to measure thickness or refractive changes on the wave guide surface. The fabrication of a channel waveguide device which integrates the splitting and combining portion of the interferometer on a glass substrate requires the fabrication of an optical waveguide. Thus, it more closely satisfies the definition of an integrated optic device. A technology to develop the optic fiber with a very small difference in refractive index between the core and the cladding was the chief goal of this project.

Silicon films containing small amounts of phosphorus is important since the difference between its refractive index and that of silicon dioxide is small enough for fabricating a single mode wave guide. Low Pressure Chemical Vapor Deposition of silicon dioxide is based on the reaction of an organic precursor, Ditertiarybutylsilane (DTBS) and oxygen. The silicon dioxide thus deposited forms the cladding for the optic fiber. By a suitable injection technique, trimethylphosphite can be injected into the reaction chamber to obtain the required amount of phosphorus in the phospho silicate glass.

1.2 Silicon Dioxide Thin Films

Chemical Vapor Deposited silicon dioxide films, and their binary and ternary alloys find wide use in VLSI processing. These materials are used as insulation between polysilicon and metal layers in multilevel metal systems, as getters, as diffusion sources, as diffusion

and implantation masks, as capping layers to prevent outdiffusion, and as final passivation layers.

Table 1.1: Properties of silica glass (Thermal Oxide)

Boiling Point(°C)	~2950
Melting Point (°C)	~1700
Molecular Weight	60.08
Refractive Index	1.46
Specific Heat (J/g°C)	1.0
Stress in film on Si (dyne/cm^3)	2-4 x 10^9, compressive
Thermal Conductivity(W/cm°C)	0.014
Dc Resistivity (Ω-cm), 25°C	10^{14}-10^{16}
Density (gm/cm^3)	2.27
Dielectric constant	3.8-3.9
Dielectric Strength (V/cm)	5-10x10^6
Energy Gap (eV)	~8
Etch rate in buffered HF (Å/min)	1000
Linear Expansion Coefficient (cm/cm°C)	5x10^{-7}

In general, the deposited oxide films must exhibit uniform thickness and composition, low particulate and chemical contamination, good adhesion to the substrate, low stress to prevent cracking, good integrity for high dielectric breakdown, conformal step coverage

for multilayer systems, low pinhole density, and high throughput for manufacturing. Some of the properties obtained for thermal oxide are shown above.

CVD silicon dioxide is an amorphous structure of SiO_4 tetrahedra with an empirical formula SiO_2. Depending on deposition conditions, CVD silicon dioxide may have a lower density and slightly different stoichiometry from thermal silicon dioxide, causing changes in mechanical and electrical film properties (such as index of refraction, etch rate, stress, dielectric constant and high electric field breakdown strength). Deposition at higher temperatures, or use of a separate high temperature post-deposition anneal step (referred to as densification) can make the CVD films approach those of thermal oxide.

Deviation of the CVD silicon dioxide film's refractive index, n, from that of the thermal SiO_2 value of 1.46 is often used as an indicator of film quality. A value of n greater than 1.46 indicates a silicon rich film, while smaller values indicate a low density, porous film. CVD SiO_2 is deposited with and without dopants, and each has unique properties and applications.

Silicon dioxide was deposited using an organic precursor, ditertiarybutylsilane (DTBS), and oxygen. DTBS has a chemical formula of $(C_4H_9)_2SiH_2$ and is a safe alternate precursor to SiH_4 with a flash point of 15°C. It is a colorless liquid with a boiling point of 128°C, vapor pressure of 20.5 torr at 20°C, and is commercially available from Olin Hunt as CONSi-4000 with a 99%+ chemical purity. This work addresses the use of this organosilane precursor for synthesizing amorphous silicon dioxide films.

1.3 Phosphosilicate Glass

The addition of small amounts of Phosphorus to silica lowers the melting point of silica glass, which can be expected to improve the overall properties of optical fibers. It is expected that the physical characteristics of the phosphorus doped silica glass are related to the chemical structure and composition of the phosphorus species in the silica network. Adding phosphorus dopant during the deposition, in the form of trimethyl phosphite(TMP), forms a phospho silicate glass (PSG). TMP is a colorless liquid with a chemical formula$(CH_3O)_3P$ with a molecular weight of 124.08 and melting point of 78°C.

Since PSG consists of two compounds P_2O_5 and SiO_2, it is a binary glass and some of its properties are considerably different from those of undoped CVD SiO_2. PSG can be flowed at higher temperatures to create a smoother surface topography, and thereby facilitate the step coverage of subsequently deposited films. The flow step is performed at 1000-1100°C, at pressures 1-25 atm, and in gas ambients of H_2O, N_2 and O_2. PSG becomes highly hygroscopic at higher phosphorus levels. Thus, it is recommended that the concentration in the oxide film be limited to 6-8 wt %P to minimize phosphoric acid formation, and consequent Al corrosion. If the PSG is to be used a s a passivation layer, the maximum permitted phophorus content is 6%.

Phosphorus content is an important factor in the fabrication of the wave guide used for the integrated device. A balance has to struck between having a high enough P content for the required refractive index and low enough lest it should become

hygroscopic. Another important aspect to be kept in mind is that excess P (above 7.5%) would make the film absorbing which is undesirable.

The concentration of phosphorus in silica glass can be measured by a dozen techniques, with a wide range of accuracy, sophistication, and effort, as summarized recently [46, 47, 48]. Wet chemical analysis yields absolute concentrations but requires considerable time and effort. The relative concentration of silica can be estimated by the index of refraction [47]. Previously the index of refraction has been determined by Raman spectroscopy, by comparing with samples of known concentrations. In short, the chemical composition of PSG can be determined by several techniques including the following: a) wet chemical colorimetry ; b) x-ray photoelectron spectroscopy; c)Fourier transform infrared spectroscopy; and d) film etch rates in buffered HF.

The following section describes the Mach Zehnder interferometer used for the integrated optical sensor. Although, this study did not focus on the actual fabrication of the interferometer, it laid the foundation for the fabrication of the interferometer.

1.4 Mach Zehnder Interferometer

The waveguide used for the Mach Zehnder interferometer consists of a 10 μm thick SiO_2 base layer obtained by Chemical Vapor Deposition. Both the core and the cladding layers were deposited by LPCVD technique. A 2μm-thick phosphosilicate glass (8 wt % P) deposited using silane, oxygen and phosphorus at a temperature of 700°C was used a core.

The optical sensor consists of a symmetric, single mode Mach-Zehnder interferometer with one arm exposed directly to the contaminated water. A glass buffer layer protects the reference arm from the influence of pollutants. Laser light is coupled into the waveguide and split into the reference and sampling arms using a Y-splitter configuration. When the active arm is exposed to pollutant molecules, there is an effective change in the refractive index sampled by that arm. Thickness changes can also occur in any hydrophobic layer which adheres to the coated arm affecting the refractive index sampled by that arm. Therefore, a phase difference, $\Delta\Phi$, develops between the active and reference arm. When light from the two interferometer arms recombine, constructive or destructive interference occurs and the light intensity exiting the interferometer, I_X, ratioed to input light. I_O, is given by :

$$I_X/I_O = 1/2\ (1 + \cos \Delta\Phi)$$

where

$$\Delta\Phi = 2\pi L(n_2-n_1)/\lambda_O$$

with L being the common length for both arms of the interferometer, n_i the effective index of arm i, and λ_O is the input light wavelength. Therefore, the phase difference is directly proportional to the effective index difference ($\Delta n_{eff} = n_2 - n_1$) between the waveguide arms. Since the pollutant level affects Δn_{eff}, then the interferometer's output intensity changes with the concentration of pollution present in the sample.

An important advantage of this sensor is its size. The distance between the interferometer's arms is on the order of 0.1 mm while the length of the interferometer is on the order of 1 cm. By placing numerous interferometers parallel to each other with

different coatings, the resultant device can be made to measure the concentration of different pollutant species simultaneously. The area of the device occupies an area no bigger than a thumb nail. Another advantage to this approach is the compatibility of the technology with standard silicon-based processing where photolithography and chemical etching steps can be used to mass produce copies of the pattern at a cost of less than a dollar per chip. For a typical arm length L = 0.6 cm, and a λ_O = 633 nm, $\Delta\Phi = \pi$ (i.e.,1 fringe shift or 100% signal modulation) for a $\Delta n_{eff} = 6x10^{-5}$. Therefore, extremely small changes in the effective index, caused by low concentrations of pollutants in the water, can be measured using this interferometric approach.

CHAPTER 2

REVIEW OF LITERATURE

2.1 Introduction

In this chapter, a review of deposition techniques of silicon dioxide and phosphorus doped silicon dioxide will be discussed. A brief review of the optical characteristics and the aim and scope of this work will be discussed.

2.2 Deposition Techniques

There are various reactions that can be used to prepare CVD SiO_2. The reason for its promising applications lies in its versatility for depositing a very large materials at very low temperatures [1]. The choice of the reaction is dependent on the temperature requirements of the system, as well as the equipment available for the process. The deposition variables that are important for CVD SiO_2 include temperature, pressure, reactant concentrations and their ratios, presence of dopant gases, system configuration, total gas flow, and wafer spacing. There are three temperature ranges in which SiO_2 is formed by CVD, each with is own chemical reaction and reactor configurations. These are :

1) low temperature deposition (300-450°C);

2) medium temperature deposition (650-750°C);

3) high temperature deposition (~900°C).

Table 2.1: Various techniques of CVD Silicon dioxide

Technique	Reactants	Remarks	References
APCVD	SiH_4, O_2	Deposition temp. 450°C, atmospheric pressure. Phosphorus doping by adding PH_3.	30
PECVD	SiH_2Cl_2, N_2O	Deposition temp. 200-350°C, N_2O:$SiCl_2H_2$ = 15:1 to 30:1.	30
PECVD	TEOS, O_2/N_2O	Deposition Temp. :400°	22-27
LPCVD	$SiH_2(C_2H_5)_2$,(Diethylsilane), O_2	Deposition temp.: 475°C, 500 mTorr pressure	31
LPCVD	TEOS, N_2O	Medium temperature range 650-800°C	43
LPCVD	SiH_2Cl_2, N_2O	High temperatures (near 900°C), 500 mTorr pressure	42

Although excellent uniformity films and properties close to thermally grown oxide can be obtained by the reaction of dichlorosilane and nitrous oxide at 900°C [2,3], the high temperature probihits the application of such approaches for deposition over aluminum-based conductors.

In the lower temperature range most of the early processes were based on the silane chemistry:

$$SiH_4(g) + O_2(g) ===> SiO_2(s) + 2H_2(g)$$

The addition of PH_3 to the gas flow forms P_2O_5, which is incorporated to the SiO_2 film to produce a phospho silicate glass (PSG). The deposition can proceed in atmospheric pressure (APCVD) reactors [4-6], low pressure CVD (LPCVD) reactors [7-21], or plasma-enhanced CVD (PECVD)[22-29]. Table 2.1 shows CVD SiO_2 obtained by different techniques and using different precursors.

Various organosilicates have been used as chemical sources in place of silane not only for generating good quality SiO_2 films and optimizing the deposition conditions, but also for safety purposes because silane is toxic, pyrophoric and potentially explosive gas. Some of these precursors are listed in table 2.2.

Table 2.2: New precursors for CVD silicon dioxide

Name	Formula	References
Tetraethoxysilane (TEOS)	$Si(OC_2H_5)_4$	7-10, 14, 15, 22-27, 32
Ethyltriethoxysilane(ETOS)	$C_2H_5Si(OC_2H_5)_3$	10-13, 16
Amyltriethoxysilane	$C_5H_{11}Si(OC_2H_5)_3$	10, 11
Vinyltriethoxysilane	$CH_2=CHSi(OC_2H_5)_3$	10, 11
Phenyldiethoxysilane	$C_6H_5Si(OC_2H_5)_3$	10, 11
Tetrapropoxysilane	$Si(OC_3H_7)_4$	13
Tetramethyicyclotetrasilane (TMCTS)	$Si_4(CH_3)_8$	20,21

Most of the work has been done with TEOS, using both LPCVD and PECVD techniques. Optimum deposition conditions and their effects on the deposit properties have been studied in detail. A rough kinetic mechanism has been proposed based on the experimental results [33].

Diehtylsilane (DES), the precursor used in previous studies, has a vapor pressure as high as 200m Torr at room temperature(25°C). DES as a suitable chemical source for CVD SiO_2 film using LPCVD technique, has been studied earlier [12,13, 16-20, 28, 29]. These studies show conformal films below 400°C, further ensured by others [12-20]. The deposition rate as a function of temperature was found to follow an Arrhenius behavior between 375-475°C yielding an apparent activation energy of 10 Kcal/mol [16]. A few experiments were carried out with DES as the Si source. Using DTBS as a precursor provided better results in terms of stress, uniformity, optical transmission and refractive index for the film to be used in the fabrication of Mach Zehnder interferometer.

The phosphorus doped silicon dioxide is usually deposited by reacting silane, phosphine, and oxygen at 300°-500°C [34-36], or by decomposition of tetraethoxysilane and triethylphosphate at 700-800°C [37]. Contamination caused by particles of silicon dioxide particles falling from loose deposits on the reactor walls is a problem for both the processes. In addition, the low temperature silane and oxygen process suffers from poor step coverage. This can be remedied by flowing the glass at higher temperatures after deposition but this requires relatively high phosphorus concentration ~6-10%.

The overall reaction for the oxidation of silane and phosphorus by nitrous oxide are assumed to be [39, 40]

$$SiH_4 + 4N_2O ===> SiO_2 + 2H_2O + 4N_2$$

$$2PH_3 + 8N_2O ===> P_2O_5 + 3H_2O + 8N_2$$

For the SiH_4 and O_2 reaction, the overall reaction can be summarized as [41]

$$SiH_4 + O_2 ===> SiO_2 + 2H_2$$

$$4PH_3 + 5O_2 ===> 2P_2O_5 + 6H_2$$

The reaction between silane and excess oxygen forms SiO_2 by heterogenous surface reaction. Homogenous gas-phase nucleation also occurs, leading to small SiO_2 particles that form a white powder on the reaction chamber walls which may potentially cause particulate contamination).

Several techniques have been used to determine the phosphorus concentration in phosphosilicate glasses. A.C Adams and S.P. Murarka[46] have compared and contrasted seven different techniques for determining phosphorus concentration in the films. Four of the measuring techniques are mutually independent: chemical analysis [47]; neutron activation; infrared absorption; and electron microprobe. The remaining three methods must be calibrated using one or more of these independent methods. A previous analysis of phosphosilicate films by neutron activation required chemical separation of the radioactive phosphorus before counting. A new technique based on refractive index was reported by A.C. Adams and S.P.Murarka [46].

Curves relating the refractive index, etch rate and sheet resistivity to the phosphorus content at constant temperature was given. A.S Tenney and M. Ghezzo [48] related the ratio of the P=O infrared absorbance band at ~1325 cm^{-1} to that of the Si-O band at ~1050 cm^{-1} to the composition of the vapor deposited phosphosilicate glasses.

2.3 Properties and Applications

Thin films for use in VLSI fabrication must satisfy a large set of rigorous chemical, structural and electrical requirements. Very low densities of both particulate defects and film imperfections such as pinholes, become critical for small linewidths, high densities, and large areas necessary for VLSI. In general, the deposited oxide films must exhibit uniform thickness and composition, low particulate and chemical contamination, good adhesion to the substrate, low stress to prevent cracking, good integrity for high dielectric breakdown, conformal step coverage for multilayer systems, low pinhole density, and high throughput for manufacturing

Table 2.3 : Properties of silicon dioxide deposited by different methods.

FILM TYPE	THERMAL	PECVD	APCVD	$SiCl_2H_2 + N_2$	TEOS
Deposition Temp(°C)	800-1200	200	450	900	700
Step Coverage	conformal	good	poor	conformal	conformal
Stress (x 10^9 dynes/cm^2)	3C	3C-3T	3T	3T	1C
Dielectric Strength (10^6 V/cm)	3-6	8	10	10	
Etch Rate (Å/min); (100:1, H_2O:HF)		400	60	30	30

Properties of silicon dioxide [44] deposited by different methods are shown in table 2.3:

The properties of doped oxide film from using different reactants [45] are shown in table

Table 2.4 : Properties of doped oxide films using different reactants.

	N_2O	O_2
Deposition Temp., °C	825	450
Deposition rate, Å/min	575	450
Composition	1.0	1.0
Etch rate, Å/min	2100	3600
Refractive index	1.445	1.445
Defect density, cm^{-2}	0.6	9.8
Junction depth, μm	1.1	1.1
Sheet resistance, Ω/sq	180	210

Both undoped and doped films of SiO_2 are easily deposited at low temperatures. Doping of SiO_2 can produce a variety of desirable film properties for some applications. Due to its poor interface qualities, CVD SiO_2 is a temporary structure if it is used in contact with single crystal silicon (e.g. as a capping layer over doped regions to prevent outdiffusion during thermal processes or as an ion-implantation mask). Its chief use, however, is a permanent structure, whose function is to increase the thickness of the field oxides, or to provide isolation between conductors. When the underlying conductor is able to withstand high temperature, one of the CVD methods may be employed due to their excellent uniformity, excellent step coverage, low particulate contamination, and

high purity. The use of SiO_2 to mask against the diffusion of the common dopants is the cornerstone of planar technology. Devices are formed by etching windows in selected areas of the SiO_2 grown on the silicon. Junctions are then formed by diffusing or ion-implanting impurities into these selected regions.

Phosphosilicate glass consists of two compounds, P_2O_5 and SiO_2; it is hence a binary glass and some of its properties are considerably different from those of the undoped oxide. PSG shows reduced stresses and is a diffusion barrier to moisture, and getters alkali ions. PSG can be flowed at higher temperatures to create a smoother surface topography, and thereby facilitate the step coverage of subsequently deposited films.

2.3 Silica-Based Single Mode Waveguides on Silicon

Low loss silica based single-mode waveguides and directional couplers have been fabricated on silicon substrates [50,51]. Silica based single-mode waveguides have a low propagation loss and an extremely low fiber coupling loss. Silica based single-mode wave guides can also be used for active optical devices such as optical switches, using temperature dependence of refractive index. Single mode channel waveguides were made from P-doped SiO_2 core layers [52]. The waveguides consisted of a 10-μm thick SiO_2 base layer by oxidizing the Si substrate in high pressure steam. A 2 μm thick phosphosiliicate glass (8 wt %) deposited using silane, oxygen and phosphene at temperature of 450°C was used a core layer. A 3 μm thick top layer of SiO_2 with 4 wt%

P was deposited using tetraethylorthosilicate, oxygen and phosphene. The resulting difference in refractive index was made use of for the Mach Zehnder interferometer. The same principle was employed in building our proposed integrated optical device.

In our experiments, the thick oxide was deposited by chemical vapor deposition using Ditertiarybutylsilane and oxygen. TMP was included for synthesizing phosphosilicate glass.

CHAPTER 3

METHODS OF THIN FILM DEPOSITION

3.1 Introduction

Thin films are used in a host of different applications in VLSI fabrication , and can be prepared using a variety of techniques. Regardless of the type of the method by which they are formed, the process must be economical, and the resultant film must exhibit the following characteristics:

1) good thickness uniformity;

2) high purity and density;

3) controlled composition and stoichiometries;

4) high degree of structural perfection;

5) good electrical properties;

6) excellent adhesion; and

7) good step coverage.

Thin film fabrication is a complicated process which involves many controlled processing parameters. The time of processing, equipment cost, throughput and quality of films are important factors for a successful commercial production. Many techniques

are available in the present technologies for film fabrication. But, most common methods that are used for economical production are physical vapor deposition (PVD) and chemical vapor deposition (CVD). This chapter describes these two methods in detail.

3.2 Physical Vapor Deposition (PVD)

In this method, thin film material in gaseous form is allowed to deposit on the substrate directly. No chemical reaction is involved in this method. All the PVD process proceed according to the following sequence of steps:

1. The material to be deposited (solid or liquid source) is physically converted into a vapor phase;
2. The vapor is transported across a region of reduced pressure (from source to substrate);
3. The vapor condenses on the substrate to form a thin film.

Depending upon the method of converting the deposition material to vapor phase, PVD is classified as: PVD by sputtering and PVD by evaporation.

3.2.1 PVD by Sputtering

Sputtering is a term used to describe the mechanism in which atoms are dislodged from the surface of a material by collision with high energy particles. Here, ions are generated

and directed at a target, the ions sputter target atoms; the ejected (sputtered) atoms are transported to the substrate where they condense and form a thin film. The advantages of this method are:

(i) Sputtering can be accomplished from large-area targets;

(ii) film thickness and its quality, like step coverage, grain structure can be controlled easily.

But, this method suffers from drawbacks such as:

(i) high equipment cost;

(ii) low deposition rate for some materials;

(iii) impurity incorporation in the film due to deposition in low-medium vacuum conditions;

(iv) inability of some materials to withstand ion bombardment resulting in degradation.

3.2.2 PVD by Evaporation

Thin films can be deposited by applying heat to the source of film material, thereby causing evaporation. If the heated source resides in a high-vacuum environment, the vaporized atoms or molecules are likely to strike the substrates (or chamber walls)

without suffering any intervening collisions with other gas molecules. The advantages of this method are:

(i) high deposition rate;

(ii) no substrate surface damage as the energy of the impinging atom is less;

(iii) high purity films can be achieved due to the deposition occurring in high vacuum. The disadvantages are:

(i) accurately controlled alloy compositions are more difficult to achieve;

(ii) *in situ* cleaning of the substrate surface is not possible;

(iii) x-ray damages, caused by e-beam evaporation processes in sputter deposition, is avoided in this method.

3.3 Chemical Vapor Deposition (CVD)

CVD is a process where one or more gaseous species react on solid surface, forming a solid phase material as one of the reaction products, the others being mostly in gaseous form. The reactant gases are introduced into the reaction chamber and are decomposed and reacted at a heated surface to form the thin film. The solid product may form a film or massive bulk on the substrate which enhances the reaction but does not undergo any chemical change. Many parameters like deposition temperature, pressure, flow rate, reactor geometry determine the nature and quality of the deposit thus produced.

Chemical and physical conditions during the deposition reaction can strongly affect the composition and structure of the product. This deposition technology has become one of the most means of creating thin films and coatings in solid state microelectronics where some of the most sophisticated purity and composition requirements must be met.

Chemical reaction types basic to CVD include pyrolysis, oxidation, reduction, hydrolysis, nitride and carbide formation, synthesis reactions and chemical transport. A sequence of several reaction types may be involved to create a particular end product. The chemical reactions may take place not only on the substrate surface (heterogeneous reaction), but also in the gas phase (homogeneous reaction). Heterogeneous reactions are much more desirable, as such reactions selectively occur only on the heated surfaces, and produce good quality films. Homogeneous reactions, on the other hand are undesirable, as they form gas phase clusters of the depositing material, which will result in poor adherence, low density or defects in the film. Thus one important characteristic of CVD application is the degree to which heterogeneous reactions are favored over homogeneous reactions. This film could be a thin film or a thick coating and should be less volatile to remain on the substrate.

3.3.1 Transport Phenomena of CVD

CVD of the film is almost always a heterogeneous reaction. The sequence of the steps in the usual heterogeneous processes can be described as follows:

1. Arrival of the reactants

a. bulk transport of reactants into the chamber,

b. gaseous diffusion of reactants to the substrate surface,

c. adsorption of reactants onto the substrate surface.

2. Surface chemistry

a. surface diffusion of reactants,

b. surface reaction.

3. Removal of by-products

a. desorption of by-products from the substrate surface,

b. gaseous diffusion of by-products away from the substrate surface,

c. bulk transport of by-products out of the reaction chamber.

The steps are sequential and the slowest process is the rate determining step. The sequential steps of deposition process can be grouped into:

(i) mass transport-limited regime;

(ii) surface-reaction-limited regime.

If the deposition process is limited by the mass transfer, the transport process occurred by the gas-phase diffusion is proportional to the diffusivity of the gas and the concentration gradient. The mass transport process which limits the growth rate is only weakly dependent on temperature. On the other hand, it is very important that the same concentration of reactants be present in the bulk gas regions adjacent to all locations of a wafer, as the arrival rate is directly proportional to the concentration in the bulk gas. Thus, to ensure films of uniform thickness, reactors which are operated in the mass-

transport-limited regime must be designed so that all locations of wafer surfaces and all wafers in a run are supplied with an equal flux of reactant species.

If the deposition process is limited by the surface reaction, the growth rate, R, of the film deposited can be expressed as $R = R_o * \exp(-E_a/kT)$, where R_o is the frequency factor, E_a is the activation energy - usually 25-100 Kcal/mole for surface process, k is the Boltzmann's constant, and T, the absolute temperature. In the operating regime, the deposition rate is a strong function of the temperature and an excellent temperature control is required to achieve the film thickness uniformity that is necessary for controllable integrated circuit fabrication.

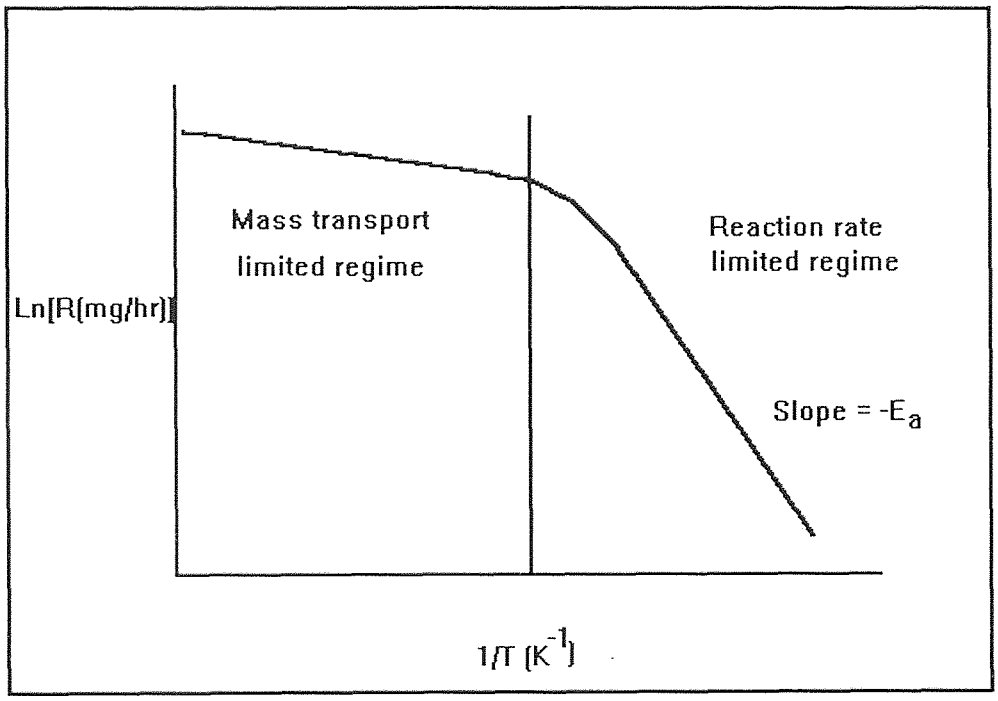

Figure 3.1 Deposition rate as a function of substrate temperature exemplifying diffusion controlled and surface-reaction controlled regimes

On the other hand, under such conditions the rate at which reactant species arrive at the surface is not as important. Thus, it is not as critical that the reactor be designed to

supply an equal flux of reactants to all locations of the wafer surface. It will be seen that in horizontal low pressure CVD reactors, wafers can be stacked vertically and at very close spacing because such systems operate in a surface-reaction-rate limited regime. In deposition processes that are mass-transport limited, however, the temperature control is not nearly as critical. Figure 1.1 shows a relatively steep temperature dependence range and a milder temperature dependence range, indicating that the nature of the rate-controlling step changes with temperature.

3.3.2 Film Growth Aspects of CVD

In general, lower temperature and higher gas phase concentration favor formation of polycrystalline deposits. Under these conditions, the arrival rate at the surface is high, but the surface mobility of adsorbed atoms is low. Many nuclei of different orientation are formed, which upon coalescence result in a film consisting of many differently oriented grains. Further decrease in temperature and increase in supersaturation result in even more nuclei, and consequently in finer-grained films, eventually leading to the formation of amorphous films when crystallization is completely prevented. Amorphous films include oxides, nitrides, carbides and glasses are of great technical importance for microelectronics applications.

Deposition variables such as temperature, pressure, input concentrations, gas flow rates and reactor geometry determine the deposition rate and the properties of the film deposit.

3.4 Types of CVD Processes

Depending upon the type of energy that is applied for the reaction to occur, CVD processes can be classified as:

(i) Plasma enhanced CVD;

(ii) Photo induced CVD;

(iii) Thermally activated CVD.

3.4.1 Plasma Enhanced CVD

In this method, gaseous reactants are allowed in a region of glow discharge created between two electrodes by electric supply. Highly reactive species are created in this region resulting in interaction between these species thus forming a solid thin film product on the substrate and electrode surfaces.

Glow discharges are usually created at low pressures in the 0.01 to 1 Torr range. This causes breakdown of molecules into the reactive species like ions, electrons. Electric field due to ac, dc or microwave sources across two electrodes creates plasma region between the electrodes. The molecules themselves can be near the ambient temperature but the breakdown electrons will be at higher temperature causing the reaction. Thus, this method can be employed at relatively low temperature and it is useful for temperature sensitive materials.

Film deposition rates are substantially higher in this method than in thermally activated LPCVD. Also, conformal step coverage can be achieved. But the disadvantage of this method is the complex process that occurs in the plasma state making the synthesis of stoichiometric films difficult. The low deposition temperature of film formation results in gases trapped in the film, which frequently causes thermal instability due to outgassing. In a newly developed method, high density plasma is created using electron cyclotron resonance ion source. The main feature of this method is low deposition temperature that is needed for high growth rate.

3.4.2 Photo Induced CVD

Short wavelength UV radiation is used to activate the reactants in gaseous phase forming the product material. A selective absorption of photonic energy by the reactant molecules or atoms initiates the process. Typically, mercury vapor is added to the reactant gas mixture as a photosensitizer and is activated by the radiation from a high intensity quartz mercury resonance lamp (253.7 nm wavelength).

The advantage of this method is low deposition temperature needed for films like SiO_2 and absence of radiation damage like the previous method. The limitation of this method is unavailability of effective production equipment.

In another type, laser beams are used for activating the reactants. In pyrolysis type reaction, a highly localized heating of the substrate that induces film deposition by CVD surface reactions, and can be exploited for the direct writing patterns on a substrate.

In evaporation method, the laser simply acts as an energy source to vaporize atoms from a target to a substrate. In yet another type, the reactant atoms or molecules absorb a specific wavelength of the laser energy applied resulting in chemical gas phase reaction that are very specific, leading to highly pure film deposits.

3.4.3 Thermally Activated CVD

This process uses direct thermal energy for the chemical reaction. The simplest type of this method is conventional atmospheric pressure CVD, where the reactant gases are allowed into the reaction chamber at normal atmospheric pressure. Energy is supplied by heating the substrate directly. The temperature and reactant flow rate determine the film growth rate. The advantage of APCVD is that it needs no vacuum pumps. The disadvantage is the tendency for homogenous gas phase nucleation that leads to particle contamination, unless special optimized gas injection techniques are used.

The deposition rate and uniformity of films created by all CVD processes are governed by the rate of mass transfer of reactant gases to the substrate and the rate of surface reaction of the reactant gases. In atmospheric CVD, these two rates are of the same magnitude. Lowering the gas pressure enhances the mass transfer rate relative to the surface reaction rate. This makes it possible to deposit films uniformly in a highly economical close spaced positioning of the substrate wafers kept vertically inside the chamber. Thus, LPCVD is a widely used in cost competitive semiconductor industry.

Another advantage of this method is that gas phase nucleation is very much reduced. This is a suitable method for SiO_2 deposition.

Depending upon the supply of energy, CVD can be further classified as hot wall and cold wall reactor system. In hot wall reactor system, the reactor is heated to high temperature and the gas molecules hitting the wall receive the thermal energy. Here the wafers are not heated directly. The advantage of this system is that a temperature gradient can be provided to the chamber which results in uniform thickness. In the other type, the wafers are heated to high temperatures directly. The reactants that are adsorbed on the surface undergo chemical change due to the temperature of the wafer. But, controlling the wafer temperature is difficult and hence uniform deposition is also difficult.

3.5 Low Pressure CVD Process

The most important and widely used CVD processes are atmospheric pressure CVD (APCVD), low pressure CVD (LPCVD) and plasma enhanced CVD (PECVD). Only LPCVD is discussed in detail below as this process is employed in this study.

Most low pressure CVD processes are conducted by resistance heating and less frequently infrared radiation heating techniques to attain isothermal conditions so that the substrate and the reactor walls are of similar temperature. The deposition rate and uniformity of the films created by all CVD processes are governed by two basic parameters:

(i) the rate of mass transfer of reactant gases to the substrate surface; and

(ii) the rate of surface reaction of the reactant gases at the substrate surface.

Lowering the pressure to below atmospheric pressure enhances the mass transfer rate relative to the surface reaction rate thus making it possible to deposit films uniformly in a highly economical close spaced positioning of the substrate wafers in the standup position.

3.5.1 Mechanism

The mass transfer of the gases involve their diffusion across a slowly moving boundary layer adjacent to the substrate surface. The thinner this boundary layer and the higher the gas diffusion rate, the greater is the mass transport that results. Surface reaction rates, on the other hand, depend mainly upon reactant concentration and deposition temperature. High deposition rates are attainable with LPCVD despite the fact that the operating total pressure is usually two to four orders of magnitude lower than atmospheric CVD. This is due to the fact that the large mole fraction of reactive gases in LPCVD, and no or little diluent gas is required. Wafer spacing has a marked effect on the deposition rate of all types of films, the deposition rate increasing linearly with increasing spacing since the quantity of available reactant per wafer increases.

3.5.2 Factors Affecting Film Uniformity

Some of the main factors affecting the film thickness uniformity in LPCVD are the temperature profile in the reactor, the pressure level in the reactor and the reactant gas flow rates. To obtain a flat thickness profile across each substrate wafer throughout the

reactor requires a judicious adjustments of these parameters. In tubular reactors, increase in temperature or pressure, increases the deposition rate upstream, thereby using up more reactant gases and leaving less to react at the downstream end; the opposite effect takes place on lowering the temperature and pressure. Similar effects occur with variations of the reactant gas flow rates at constant gas partial pressure, or with changes in the size and number of the wafers processed per deposition run. The uniformity of thickness and step coverage of these films are very good. These films have fewer defects, such as particulate contaminants and pinholes, because of their inherently cleaner hot wall operations and the vertical wafer positioning that minimize the formation and codeposition of homogeneously gas phase nucleated particulates.

Most of these chemical reactions are endothermic and of different types such as pyrolysis, decomposition, oxidation, reduction, chemical transport reaction, etc. The process should have the following sequential steps for completion:

1) Mass transport of reactants to substrate

2) Adsorption of reactants on substrate surface

3) Chemical reaction on the surface

4) Desorption of the product gases from the surface.

5) Mass transport of product gases away from substrate

CVD processing has several advantages over other methods of film deposition. These advantages make it one of the popular methods adapted commercially. These are listed below:

1) Conformal step coverage can be achieved by this method. It is an important factor for the fabrication of electrical devices.

2) Stoichiometric control of the film can be easily achieved by adjusting the processing parameters like deposition temperature, flow rates, etc.

3) High throughput is possible, especially by LPCVD, due to reactor structure and enhanced mass transfer of the reactant.

4) The quality of the film can be easily reproduced by this method because the processing parameters can be repeated without difficulty.

5) Since the whole area of the substrate is equally exposed to the reactants, good uniformity of film thickness can be achieved.

6) Selective deposition of film onto the substrate can be done by masking unwanted portions of the substrate.

7) Unlike in PVD, there is no radiation like e-beam involved, therefore, there is no possibility of damage of substrate or the film, by this method.

8) CVD offers an excellent opportunity of impurity doping in device fabrication. This is possible by simply mixing the required dopant along with the reactants.

9) Low maintenance cost of the equipment makes it an attractive method for large scale production.

3.6 Summary

The common methods of film deposition, namely PVD and CVD, were described. Their classification, advantages and disadvantages were mentioned. The LPCVD was found to be suitable method due to its advantages over APCVD. Therefore, in this study, hot wall pressure chemical vapor deposition system was employed.

CHAPTER 4

EXPERIMENTAL SETUP AND CHARACTERIZATION TECHNIQUES

4.1 Introduction

Silicon dioxide and phosphorus doped silicon dioxide thin films were synthesized in a LPCVD reactor altering various parameters like temperature, gas composition and time of deposition. Fourier Transform Infrared analyses were done on the synthesized films to detect presence of phosphorus in the deposited films. Refractive Index and thickness of the films were measured by using ellipsometry and interferometry respectively. The optical transmission of the films was measured using a UV spectrophotometer. The current-voltage, capacitance-voltage, resistivity and the dielectric constants of the films were measured.

4.2 LPCVD Reactor

The schematic for hot wall low pressure chemical vapor deposition reactor is shown in Fig 4.1. The reactor consists of fused quartz tube of 5 inches in diameter and about 50 inches in length. The tube is kept inside a Lindbergh three zone surface. The zone temperatures are controlled by manual settings. A maximum temperature of 1200°C can be reached using this furnace and a gradient of temperature can also be obtained inside the quartz tube. Heating is provided by Lindbergh silicon carbide heating elements. It is

equipped with Plantinel II thermocouples which sense the temperature of the zone and the voltage developed which is used for automatic temperature control. The tube and the coils are surrounded with a ceramic enclosure. The tube is sealed on both the ends by end caps and metallic rings. During the heating process, thermal expansion of the O-rings may cause leakage in the system. To avoid this problem, water cooling is arranged by cold water circulation. Apart from this, additional cooling is provided by fans. A MKS baraton gauge with a range of 10 Torr is used to monitor the pressure at the input end. The monitored pressure is displayed by the MKS display unit. The input seal consists of three provisions for gas inlet, so that if more than one precursor is used, they will mix together and diffuse inside.

The system is kept at low pressure by vacuum pumps. This system uses a booster pump and a mechanical backing pump. The booster pump is used to enhance the flow of gases and thereby the pumping speed. Mechanical backup does the real pumping and the combination provides a vacuum as low as a milli Torr. The booster pump is a *Ruvac* single stage roots pump operated at 220 V supply and the backing pump is a *Trivac* dual stage rotary vane pump. Nitrogen ballast gas is used in the pump to dilute any hazardous outgoing gas. An oil filtration system is also used to separate the micron size dust particles that are accumulated during the pumping process.

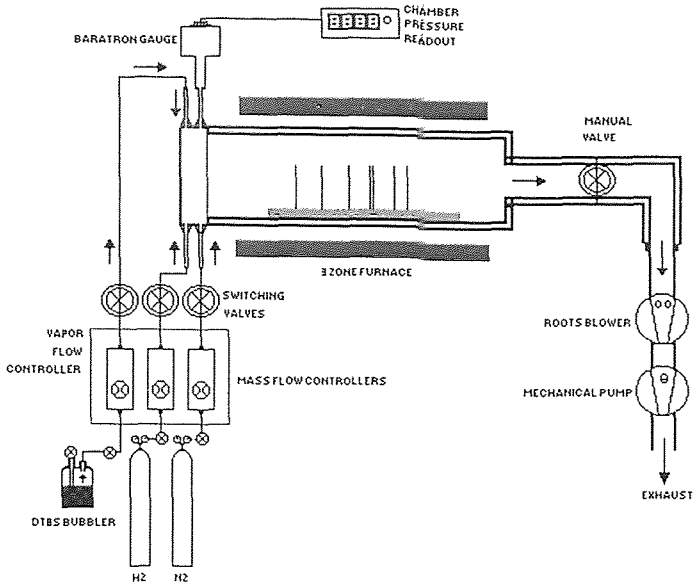

Figure 4.1 : A schematic of the LPCVD reactor

Wafers are loaded inside the tube using a quartz carrier boat. Wafers are kept vertically in the slots provided in the boat. The boat is kept inside the quartz tube and the tube is sealed by the inlet lid. A manual control valve is provided at the output end to control the rate at which the gas is removed from the reactor. Precursor is allowed through a pneumatic control valve provided at the input end. Unloading of the wafers is done by bringing the reactor to atmospheric pressure. This is done by closing the valve and passing a controlled flow of nitrogen into the chamber.

4.3 Experimental Setup

4.3.1 Flow Rate Calibration

CVD reactors and other process systems require that the rates of introduction of the process gases into the process chambers be controlled. In some applications, this is achieved by adjusting the gas influx to maintain a constant chamber pressure. More commonly, the process gas flow is directly controlled. To do this, mass flow controllers are used. Mass flow controllers consist of a mass-flowmeter, a controller, and a valve. They are located between the gas source and the chamber, where they can monitor and dispense the gases at predetermined rates. The operation of a thermal mass flowmeter relies on the ability of a flowing gas to transfer heat. the mass flowmeter consists of a small sensor tube in parallel with the larger main gas flow tube. A heating coil is wrapped around the sensor tube midway along its length, and temperature sensors are located upstream and downstream of the heated point. When the gas is not flowing, and the heat input is constant, the temperatures at both sensors are equal. Flowing gas causes the temperature distribution in the sensor to change. It can be shown that the mass flow, m_f, is given by:

$$m_f = (\kappa\, W_h\, \Delta T)^{1.25}$$

where W_h is the heater power, ΔT is the temperature difference between the points where the sensors are located, and κ is a constant that depends on the heat transfer coefficients, the specific heat of the gas, the density of the gas, and the thermal conductivity of the gas. Mass rate can be thus measured by the temperature difference.

Gas flows were controlled by Applied Materials model AFC 550 automatic N_2 mass flow controllers which were corrected for DTBS and O_2 flows. The pressure in the reactor was measured with a barratry gauge from MKS. The N_2 calibration of the AFC was checked by delivering a fixed volume of gas (product of the metered flow rate and time) into the known reaction chamber volume. The pressure increase was measured and used to calculate the volume of the gas corrected to the standard condition. (0°C, 1 atm). According to the gas law, the flow rate corrected to STP (sccm) is given by the formula below:

$$\text{Flow Rate} = 60(\Delta P/\Delta t)(T_0 V/P_0 T)$$

where ΔP = pressure increase in Torr,

$T_0 = 273$ K

$P_0 = 760$ Torr

V = volume of the chamber, cm^3

Δt = time of delivering gas, sec.

Routine flow rate calibrations were conducted before every run.

4.4 Deposition Procedure

Wafers were loaded inside the tube using a quartz carrier boat. Wafers are kept vertically in the slots provided on the boat. The boat is kept inside the quartz tube and the tube is

sealed by inlet lid. A manual control valve is provided at the output end to control the rate at which gas is removed from the reactor and therefore controls the pressure inside the reactor. Precursor is allowed through a pneumatic control valve provided at the input end. Unloading of the wafer is done by bringing the reactor to atmospheric pressure. This is done by closing the output valve and passing a controlled flow of nitrogen into the chamber. Films were deposited on <100> oriented single sided polished wafers, and fused quartz wafers. Single side polished wafers are 10cm in diameter, 525 μm in thickness, labeled and weighed by electronic weighing balance. The wafers were placed at either 3 cm or 5 cm distance from each other. The boat was placed at a distance of 64 cm from the door.

After loading, the furnace was brought to low pressure by pumping down the chamber. The temperature was raised to the required level slowly in steps of about 250°C. The temperature was allowed to reach the set value in all the three zones before raising it further until the desired value is reached.

Once the required temperature was reached, the valves for oxygen flow were opened. When the flowmeter showed stabilized value of flow, the DTBS and TMP tanks were opened. The pressure was then set to the required value. Care was taken not to let the organic precursors into the chamber before there was oxygen flow lest the films should have carbon in them. The oil filter was switched on during deposition.

4.4 Characterization of SiO_2 and Phosphosilicate Glass Films

4.4.1 Thickness

Film thickness was measured by Nanospec interferometer which consists of an entrance slit mirror located at the designed focal length of the objective lenses of the Olympus BH microscope used with the instrument. The estimation is based on the monochromatic light interface fringes formed from the sample surface. The device consists of Nanometrics Nanospec/AFT microarea gauge and SDP-2000T film thickness computer. The thickness of the film deposited on the wafer was measured at five different points. The refractive index provided was first estimated, as for silicon dioxide, 1.46 is the typical value. Thickness was measured at five different points on the wafer. Deposition rate was determined as the film thickness over the deposition time, and averaged over all the wafers in the run.

4.4.2 Refractive Index

The refractive index was determined by a Rudolph Research Auto EL ellipsometer, which consists of a polarizer and a compensator. Plane (45°) polarized light the polarizer is elliptically polarized when it passes through the compensator. It is then reflected by the sample surface, collected by a detector, analyzed for its intensity, and finally quantified by a set of delta psi values. The values were then fed to a computer which numerically solves an equation to give the refractive index of the film. The refractive

index of the film deposited on the wafer was measured at five different points and then averaged out to the refractive index of the wafer.

4.4.3 Infrared Spectra

The levels of interstitial oxygen and phosphorus were determined by using infrared absorption spectroscopy. The analysis was done on a Perkin-Elmer 1600 series FTIR spectrophotmeter to determine the characteristics of the deposits. A spectrum of percent transmittance or absorption was obtained for samples of known thicknesses.

The composition of phospho silicate glass can be analysed by infrared absorption plot. The ratio of the intensity of the P=O absorbance band at ~1325 cm^{-1} to that of the Si-O band at ~1050 cm^{-1} can be correlated with the composition of vapor deposited phospho silicate glasses over the range 0-20 mol per cent P_2O_5.

The properties of PSG which make it useful in a given application may depend on its composition. Hence, it must be possible to determine and control this composition. Composition control is usually achieved by controlling the temperature and reactant gas composition during the CVD of the PSG film. Composition determinations based on the IR spectra of vapor deposited borosilicate and arsenosilicate glasses have proven useful. The IR reflectance spectra of silicate glasses have been employed as a qualitative test for the presence of phosphorus oxide. Tenney and Ghezzo[48] have proposed a method to determine compositions of PSG. From the infrared plot, the linear absorption ratio for the glass (ratio of the linear absorption of PSG to that of pure SiO_2) is calculated. This

ratio as a function of the glass composition for different temperatures was plotted by Tenney et al [48]. Based on their results, a calibration curve was plotted for 700°C.

A similar approximation for the P=O band area and a corresponding calibration curve was obtained. An average of both the methods was used to obtain the phosphorus content in the given glass.

4.4.4 Stress

The stress in the film was determined by a house developed device, employing a laser beam equipment which measures change in radius of curvature of the wafer resulting from the film deposited on one side. Two fixed and parallel He-Ne laser beams were incident on the wafer surface before and after deposition. The reflected beams from the two surfaces was then projected by an angled plane mirror as two points onto a scale in a certain distance, and thus, their separation can be measured more accurately. The change in separation of these two points was fed into Stony's Equation to obtain actual stress value. The calculation formula is:

$$\delta = 12.3\ D/T$$

where D = distance difference between two points before and after deposition (mm);

T = thickness of the films, (λm);

δ = stress of the film (Mpa), negative value indicates compressive stress

CHAPTER 5

RESULTS AND DISCUSSION

5.1 Introduction

The results of silicon dioxide and phosphosilicate glass thin films synthesized on Si and quartz substrates at a constant pressure of 0.2 Torr, at different temperatures between 700°C and 850°C, and at various flow rates of oxygen, DTBS and TMP are presented in this chapter. Thick oxide (10μm thickness) runs were carried out to fabricate the buffer layer for the waveguide in the Mach Zehnder interferometer. The distance between the wafers was also varied to study the deposition rate as a function of the distance and to get uniform films.

5.2 Silicon Dioxide Thin Films

5.2.1 FTIR Analysis

The figure shows the FTIR spectrum of SiO_2 in the range of 4000 cm^{-1} to 400 cm^{-1} for the oxide deposited at 700°C. The figure shows peaks at 1060, 800 and 440 cm^{-1} corresponding to stretching, bending, and rocking modes respectively.

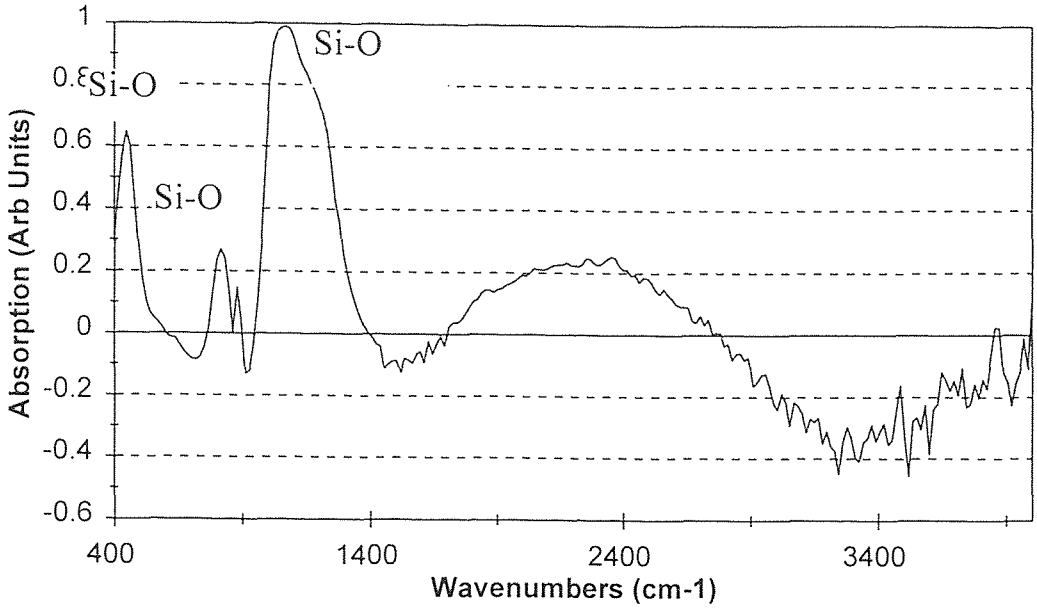

Figure 5.1: FTIR spectrum for silicon dioxide

5.2.2 Deposition Rate Analysis

One of the most important aspects of film growth is the rate of film growth with respect to the deposition temperature. Since a chemical reaction is involved in the formation of the film, the rate of the chemical reaction is a key factor for deposition rate. The rate of chemical reaction depends upon the deposition temperature. The purpose of this study is to evaluate the growth rate and characterize the silicon dioxide films deposited using ditertiary butyl silane. SiO_2 films were deposited at different temperatures from 700°C-850°C while the other parameters like pressure flow rate, deposition time and wafer spacing were kept constant. Another study carried out at 700°C with pressure and wafer

spacing constant, varied the flow rates of oxygen. A third study was done varying the wafer spacing, other parameters remaining constant.

The temperature dependence of the rate has been found to fit the expression proposed by Arrhenius:

$$\text{Growth Rate (G.R)} = A\exp(-E_a/RT)$$

where,

A is the pre-exponential factor (nearly independent of temperature);

E_a is the apparent activation energy of the chemical reactions;

R is the gas constant and is equal to 1.98717 cal $K^{-1}mol^{-1}$;

T is the absolute temperature of the reaction (K);

Taking natural logarithm (Ln) on both sides of the above equation, and plotting a graph of Ln growth rate versus reciprocal of temperature, leads to a straight line with a negative slope. This type of curve is called the Arrhenius plot. The negative slope of the curve gives the ratio between the activation energy and gas constant. By determining the slope of the curve, the activation energy for the reaction can be calculated. Figure 5.2 shows Ln of growth rate (in Å per minute) plotted against the reciprocal of deposition temperature in Kelvin scale. The experiments were carried out between temperatures of 700 and 850°C; DTBS flow rate of 10 sccm and O_2 flow rates of 50 and 100 sccm; pressure of 0.2 Torr. Beyond 800°C, growth rate decreased slightly as the temperature was increased. At temperatures above 800°C, the deposition rate was observed to

decrease reflecting a combination of factors including the transition into mass-transfer limited regime and the adsorption of decomposition products which act as retardants to the growth process. Between 700°C and 800°C, the slope of the curve was found to be -2.44 giving an activation energy of about 4.8 KCal/mol for the 5 to 1 flow ratio of oxygen and DTBS and was found to be -0.66 giving an activation energy of 1.25 KCal/mol for the 10 to 1 flow ratio of oxygen.

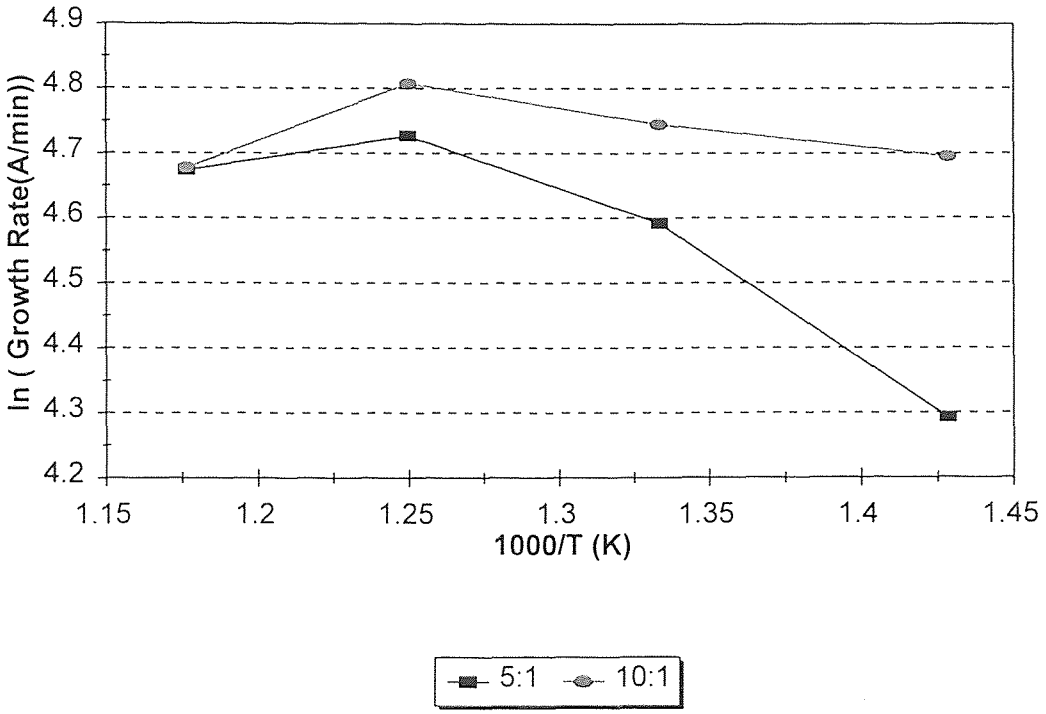

Figure 5.2 Variation of growth rate as a function of Temperature at different flow ratios of O_2 and DTBS (O_2:DTBS = 5:1 and 10:1)

Figure 5.3 shows a plot of deposition rate as a function of distance between the wafers. It was observed that as the distance between the wafers was increased from 2 cm to 5 cm the deposition rate increased. This is not unusual since the increase in distance

exposed the wafers to the reactant gases to a larger extent and thus, deposition and uniformity of the deposit were favored.

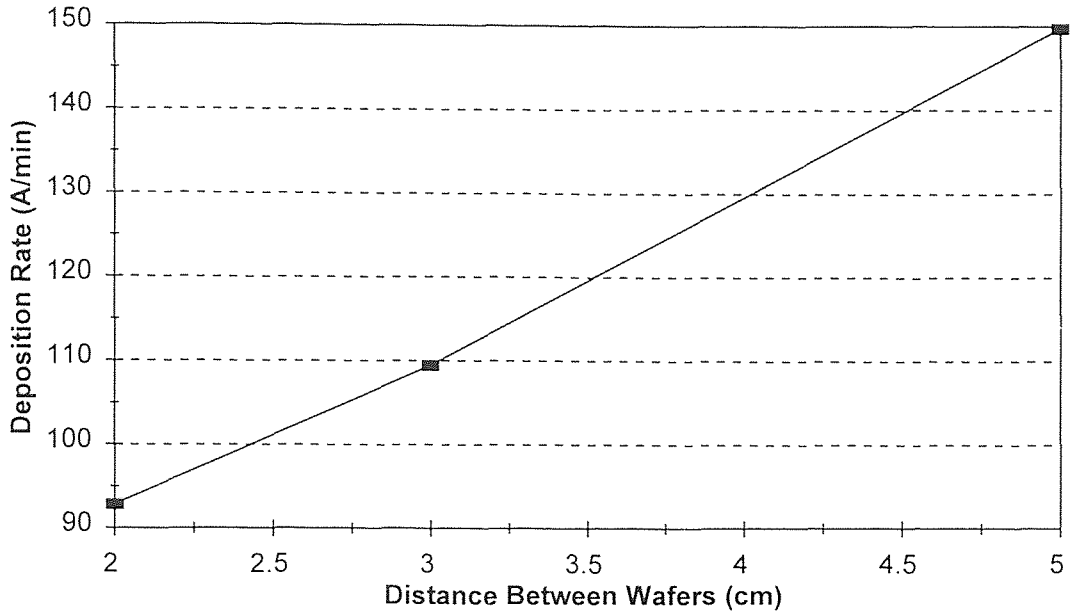

Figure 5.3: Variation of average deposition rate as a function of distance between the wafers.

5.2.3 Refractive Index Analysis

Figure 5.4 shows the variation of refractive index as a function of various temperatures at flow ratios of oxygen to DTBS of 5 to 1 and 10 to 1 and at a fixed pressure. The refractive index of the deposits was determined by using a Rudolph Research Auto EL Ellipsometer at five different points. The average was then taken for plotting.

The refractive index showed increase with increase in temperature of deposition. It is suspected that at higher temperatures, the composition of the deposits changed to

carbon rich. Decrease in optical transmission with increase in deposition temperature also suggested presence of carbon in these films. A carbon rich film shows increase in refractive index due to the high inherent refractive index of carbon.

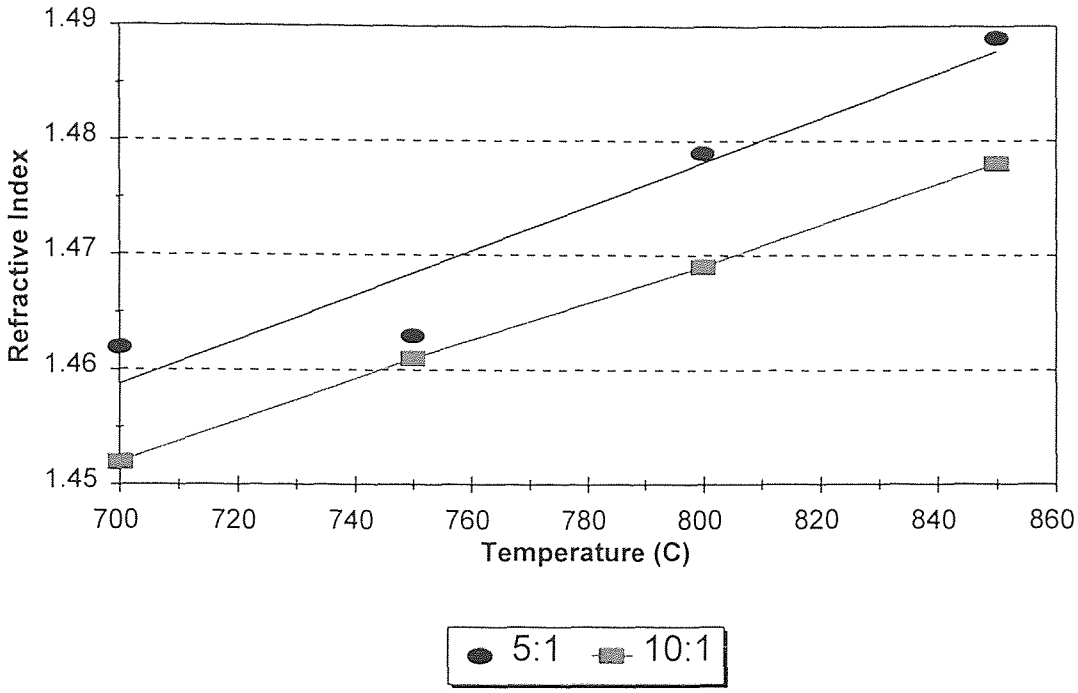

Figure 5.4: Refractive Index vs. Temperature for different flow ratios of oxygen and DTBS

The figure also shows that with higher oxygen flow, the refractive index was lower and closer to that of the thermal oxide further establishing the fact that at lower oxygen flow rates, carbon content in the films was higher. The refractive index showed a linear dependence on temperature. Deviation was observed when the flow ratio of oxygen to DTBS was 5:1. This could not be explained clearly. However, the curve was approximated by a linear fit. The plot shows that the two lines corresponding to two different flow ratios of oxygen and DTBS were parallel with roughly the same slope .

5.2.4 Stress Analysis

Analysis of stress with respect to temperature showed that the stresses were remained very low through the entire regime of deposition temperatures. The stresses were low tensile at lower temperatures and became less tensile as temperature was increased from 700° to about 750°C , beyond which they tended to be increasingly compressive.

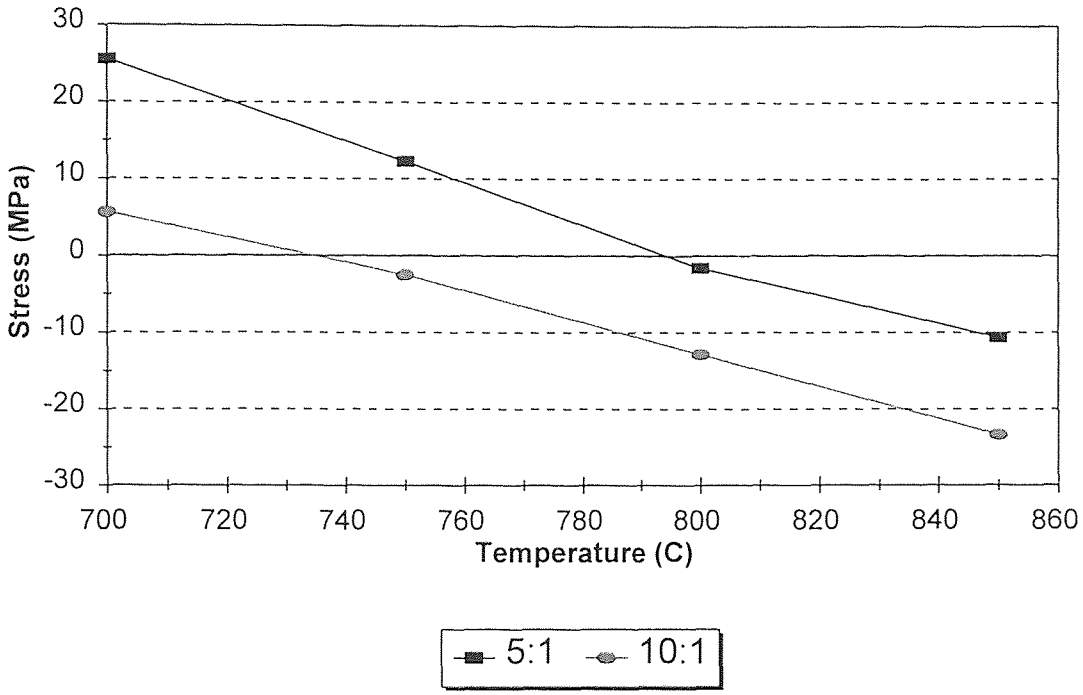

Figure 5.5: Stress as a function of temperature for different flow ratios of oxygen and DTBS (Oxygen: DTBS).

Stress can result from differences in thermal expansion coefficients (α) of the film and the substrate. Higher temperatures result in some stress relief and the stresses tend to be more compressive [1]. Also, the presence of carbon (α=3.8 x 10^{-6} K^{-1}) causes a positive difference in the thermal expansion coefficients resulting in stresses being compressive.

5.2.5 Optical Transmission

The optical transmission for the silicon dioxide is shown in figure 5.6. The film was almost 98 percent transparent above a wavelength of 500nm. This implied that the film could be used in the fabrication of the waveguide for the interferometer.

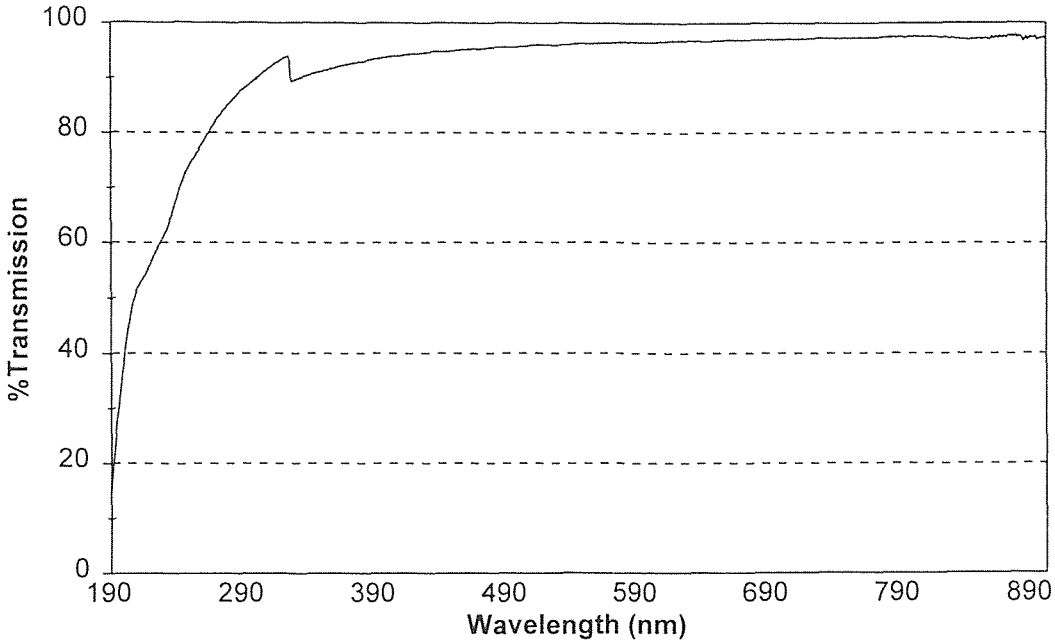

Figure 5.6 : Optical transmission spectrum for silicon dioxide.

5.3 Phosphosilicate Glass

5.3.1 FTIR and Compositional Analysis

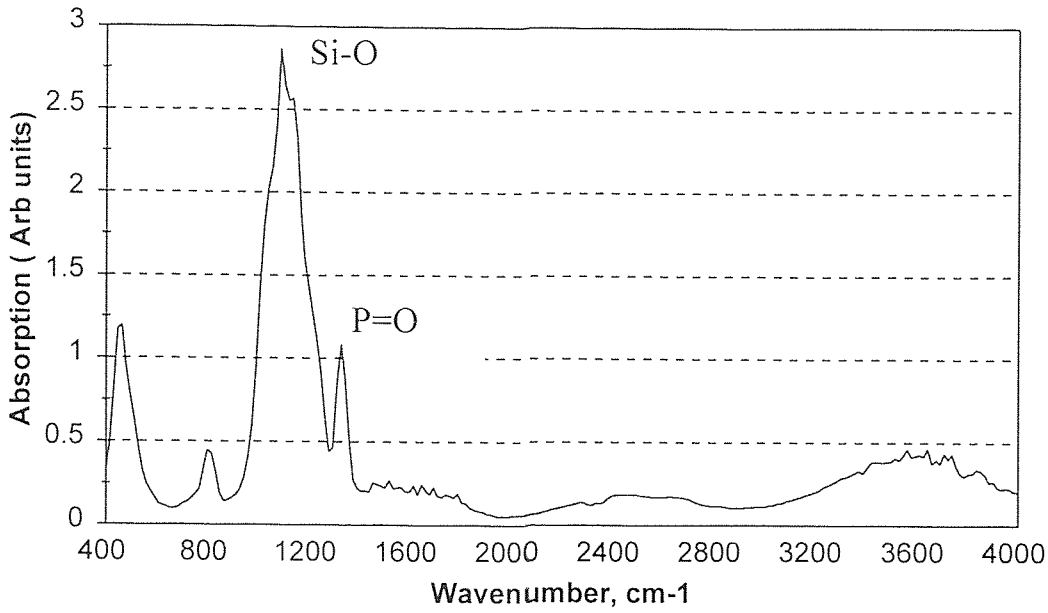

Figure 5.7 :FTIR spectrum of phosphosilicate glass showing peaks for SiO_2 and P-doped SiO_2

The following figures show FTIR spectra showing peaks for different percentages of phosphorus. The different percentages of phosphorus were obtained by varying the TMP flow rate as explained in chapters 2 and 4. An appropriate percentage of phosphorus was necessary to obtain the properties, especially the refractive index, for the fabrication of the interferometer. The phosphorus content was measured based on work done by Tenney and Ghezzo [48].

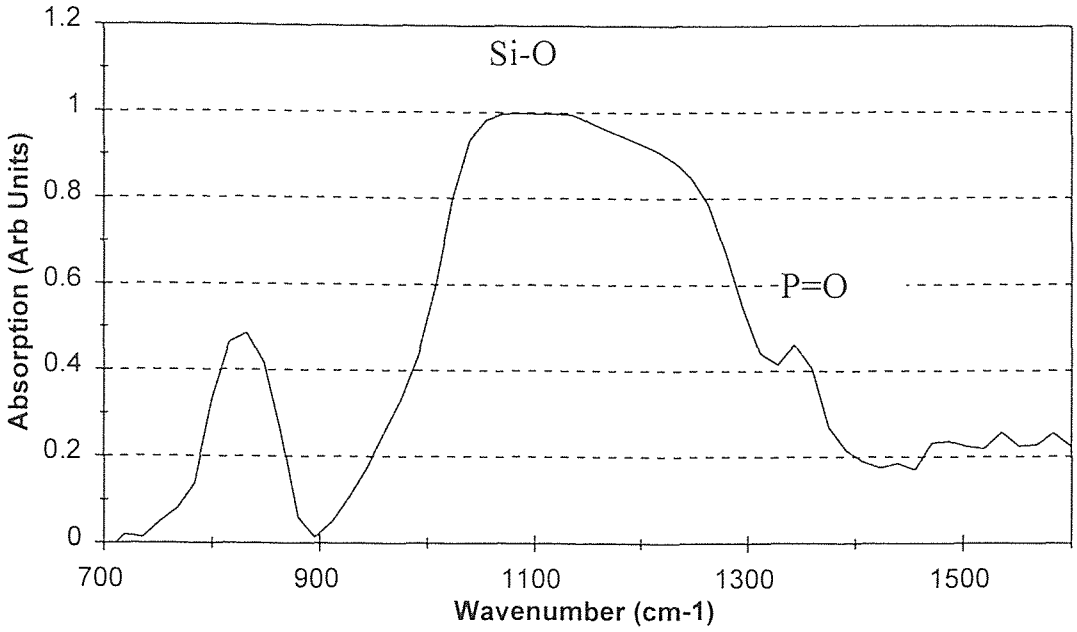

Figure 5.8 : FTIR spectrum of PSG showing 2.4 percent phosphorus.

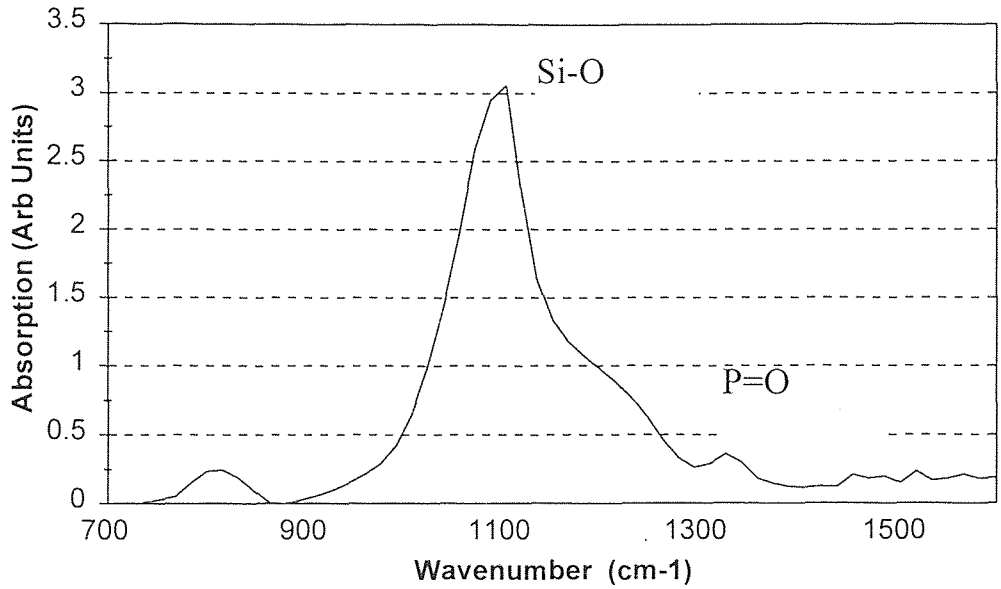

Figure 5.9 : FTIR spectrum of PSG containing 5 percent phosphorus

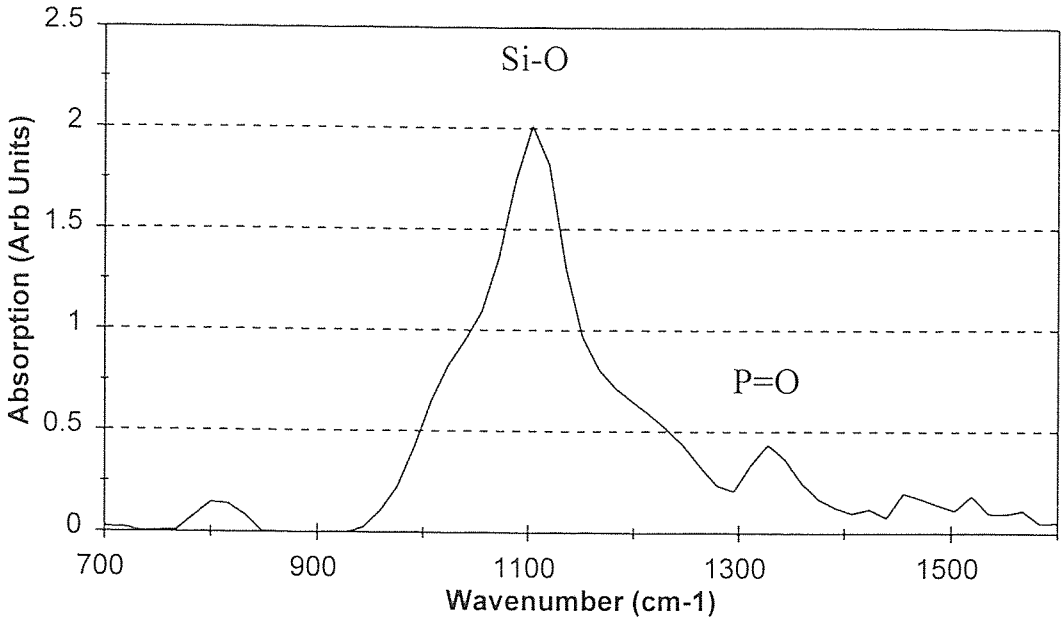

Figure 5.10: FTIR spectrum of PSG containing 8 percent phosphorus.

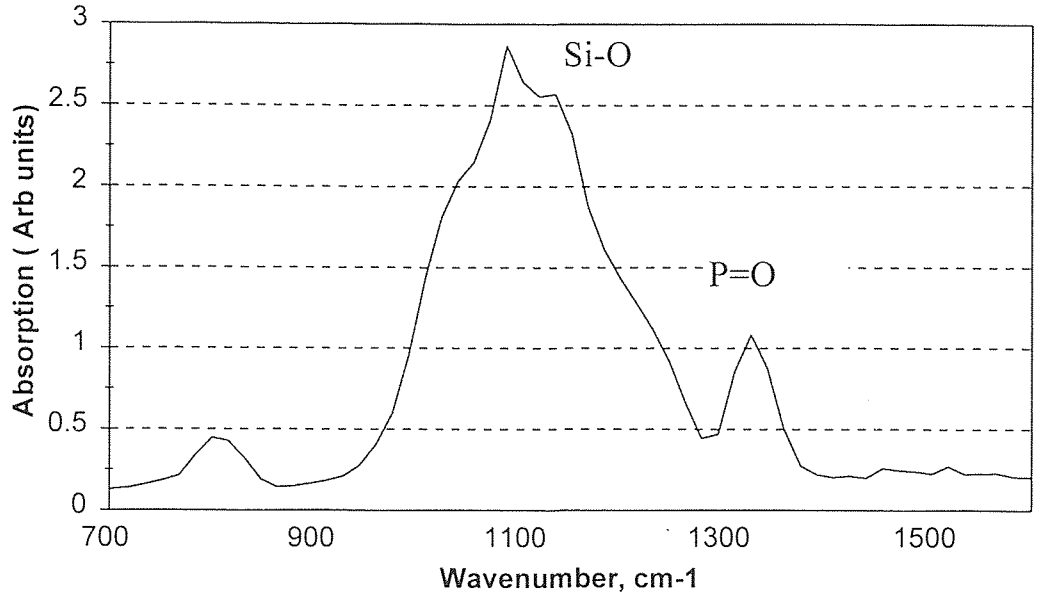

Figure 5.11: FTIR spectrum of PSG containing 16.6% phosphorus

5.3.2 Deposition Rate Analysis

The deposition rate for the phosphosilicate glass was found to increase with increase in the TMP flow, in other words, increase in phosphorus content.

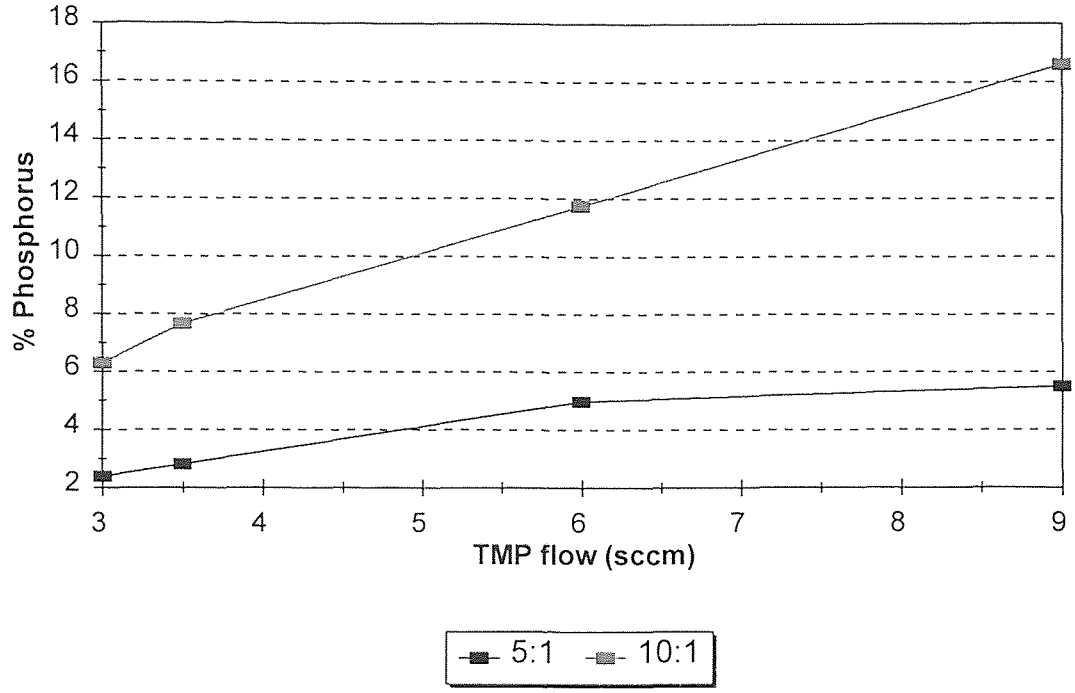

Figure 5.12 : TMP flow rate vs. obtained phosphorus content in the deposit for different flow rates of oxygen and DTBS (Oxygen : DTBS)

The deposition rate is proportional to the phosphorus concentration. It appears that the deposition rates and the weight percent P are related to the gas flow rates.

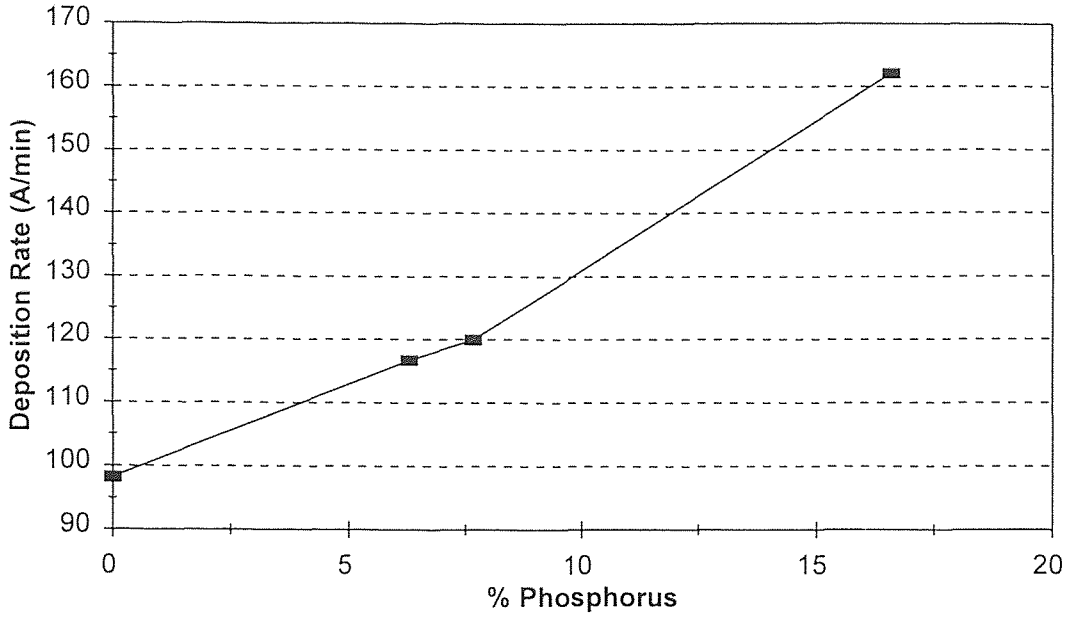

Figure 5.13 : Variation of deposition rate with weight percent phosphorus in phosphosilicate glass.

The effects of gas flow of the film uniformity can be studied; the percentage variation being defined as the maximum value of the thickness minus the minimum value divided by the average value. The films obtained were fairly uniform and so this analysis was not done.

5.3.3 Density Analysis

The film density is calculated as the ratio of the weight gained by the film to the thickness of the film for that particular wafer. The thicknesses used were based on the values obtained by Nanospectrophotometer. It was observed that the density increased as the TMP flow was increased (Figure 5.9). The hump in the density curve could not be

comprehended. However, the data was not verified by carrying out the experimental run to reproduce the data.

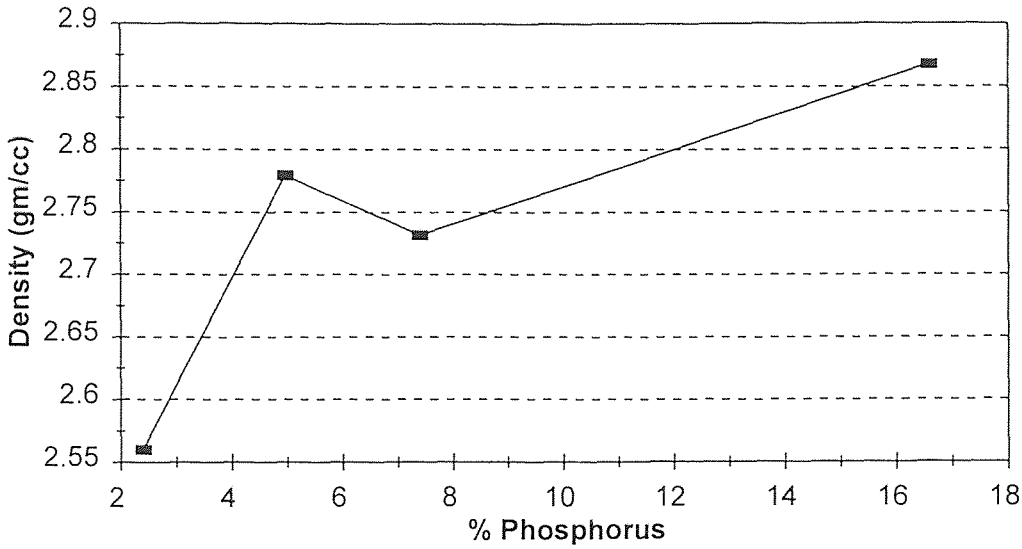

Figure 5.14 : Density vs. phosphorus content.

5.3.4 Stress Analysis

Stress was determined using a Laser Stress Analyser. Stress determined was plotted as a function of phosphorus concentration and is shown in figure 5.13. It was observed that the stress became more and more compressive as the phosphorus content in the film increased. Phosphorus has a very high coefficient of thermal expansion. This causes the residual stresses to be compressive.

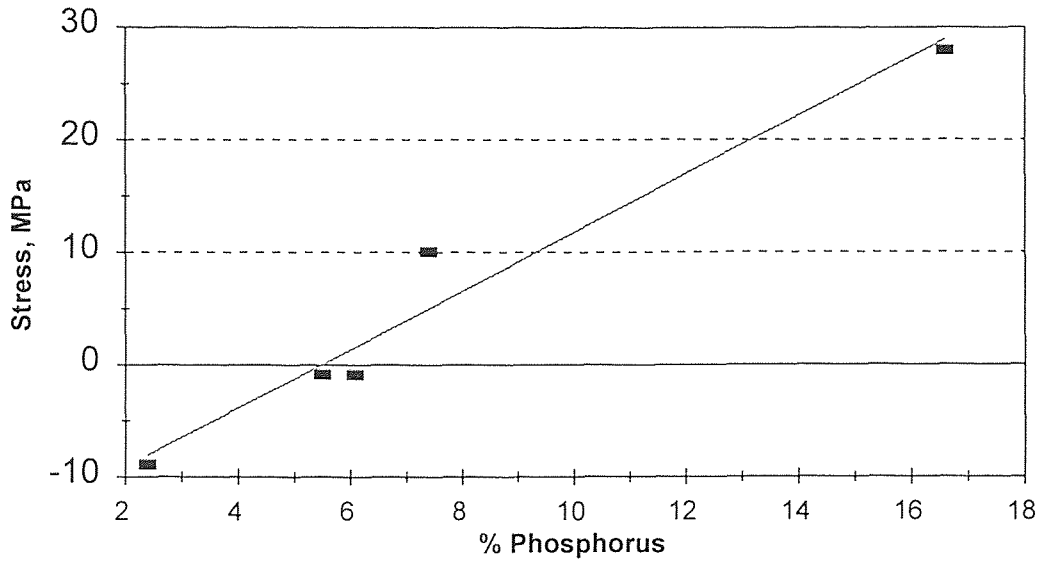

Figure 5.15 : Stress vs. phosphorus content in PSG.

5.3.5 Refractive Index Analysis

The refractive index seemed in increase with phosphorus content. Silicon dioxide containing small amounts of phosphorus are frequently used in silicon integrated circuits as the physical properties are improved with this small addition of phosphorus. The

slightly higher refractive index of phosphorus is useful because it can be used in the fabrication of the optical waveguide for the Mach Zehnder interferometer. A plot of the refractive index as a function of phosphorus concentration is shown in figure 5.16.

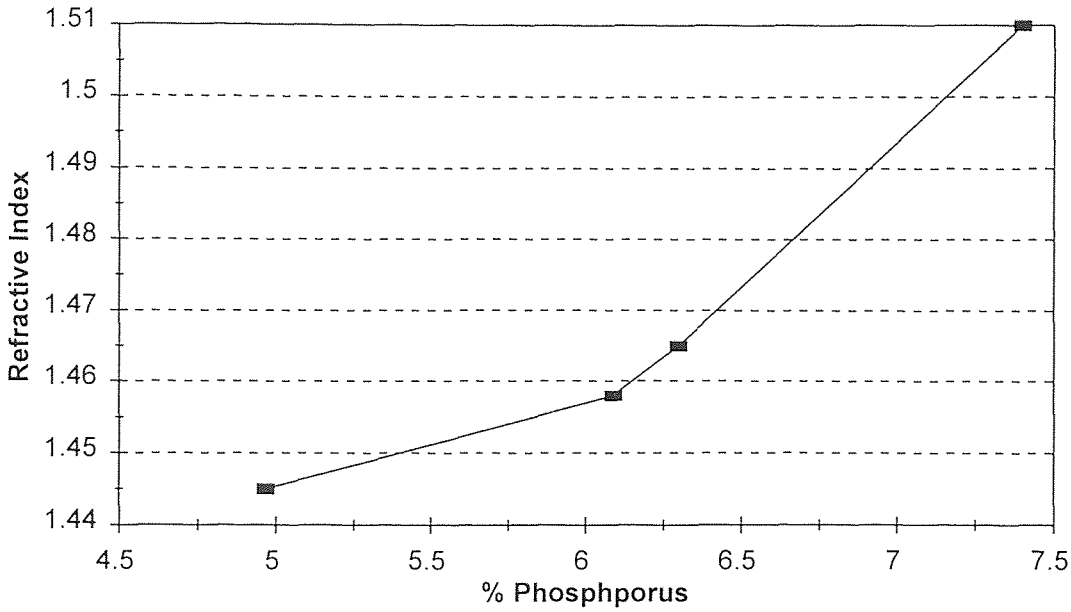

Figure 5.16 : Refractive index vs. weight percent phosphorus in PSG

P_2O_5 present in silicate glasses behave as network modifiers and cause a change in structure. This could possibly account for the increase in refractive index.

5.3.6 Optical Transmission

The optical transmission for the phosphosilicate glass was measured using a UV-spectrophotometer(Figure 5.15). The result showed that a near perfect transparent film was obtained. Optical transmission is an important property to be considered for building the interferometer. A 99 percent transmission at 630 μm wavelength showed that the

phosphosilicate glass obtained from vapor deposition of DTBS, TMP and oxygen was an excellent core material for the waveguide

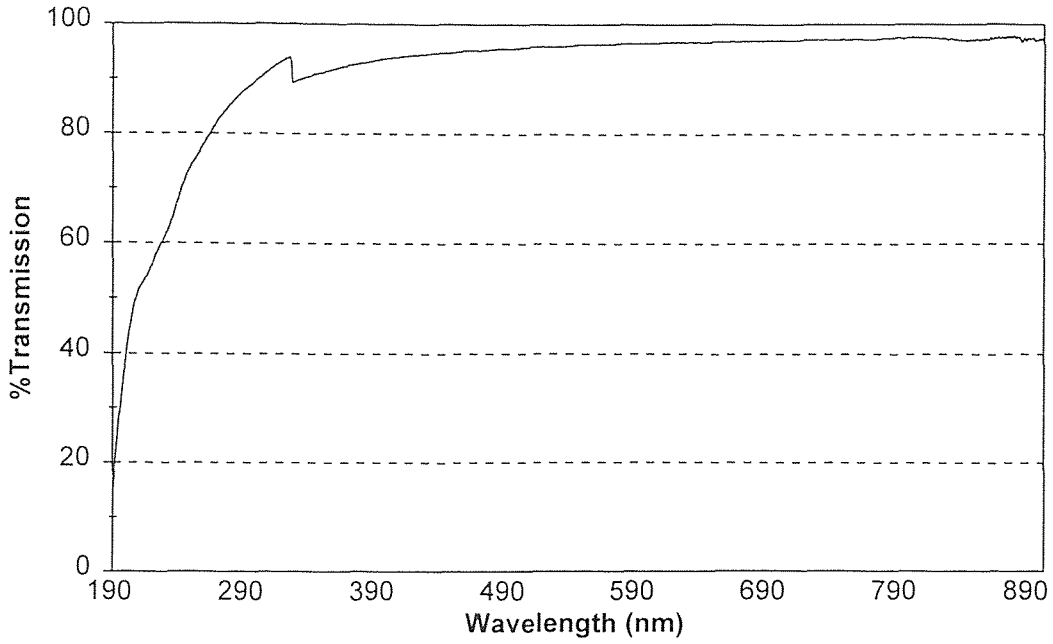

Figure 5.17 : Optical transmission spectrum for phosphosilicate glass.

5.4 Summary of Results

The following tables show a summary of results of the experiments carried out to fabricate silicon dioxide and phosphosilicate glass thin films. The optical transmission was almost 99% in both the cases. The FTIR spectrum for SiO_2 showed peaks for the Si-O bond at 1060, 800 and 440 cm^{-1} corresponding to stretching, bending, and rocking modes respectively. The FTIR spectrum for the phosphosilicate glass showed a peak for the P=O bond at 1323 cm^{-1}.

Table 5.1 : Summary of results for silicon dioxide thin films by CVD of DTBS and oxygen

Deposition Temperature (°C)	Flow Ratio ($DTBS:O_2$)	Deposition Rate (Å/min)	Stress (MPa)	Refractive Index
700	50:10	107	-25	1.462
750	50:10	113	-12.5	1.463
800	50:10	98.7	3.2	1.479
850	50:10	73.2	10.5	1.489
700	100:10	107.51	-5.7	1.452
750	100:10	122.5	2.5	1.461
800	100:10	115	12.5	1.469
850	100:10	109.49	23.2	1.478

Table 5.2 : Summary of results for phosphosilicate glass thin films by CVD of DTBS, TMP and oxygen

Wt. % Phosphorus	Stress (5:1), (MPa)	Stress (10:1), (MPa)	Deposition Rate (10:1), (Å/min)	Density (gm/cc) (10:1)	Refractive Index (10:1)
2.4	-8.856	-8.5	102.4	2.56	1.423
5.5	-.845	0.03	107.8	2.78	1.452
6.09	-.86	1.56	116.8		1.458
7.4	10.26	4.98	120	2.73	1.51
16.6	28	28.96	162.1	2.868	

CHAPTER 6

CONCLUSIONS

Silicon dioxide and phosphorus doped silicon dioxide thin films processed in this study were amorphous and uniform. The undoped oxide showed increasing refractive index with increasing deposition temperature and was probably carbon rich at higher deposition temperatures. The stresses were very low tensile(-25 MPa) and became compressive as the temperature increased. In the case of binary glass, the refractive index and density increased with increasing phosphorus content. The stresses were compressive and tended to become progressively compressive with increasing phosphorus content. The optical transmission was almost 99% at 700°C for both undoped and doped oxides. The refractive index for the undoped oxide at 700°C was 1.459 and for the doped oxide with 7.5 % by weight of phosphorus, it was 1.483. This refractive index difference was optimal for the fabrication of the Mach Zehnder interferometer.

The exact phosphorus content should be measured by other techniques. An empirical method was adopted to measure the phosphorus content in our study.

REFERENCES

1. Coulson, A.R; Tauber, R.N., In *Silicon Processing for the VLSI Era*; Wolf, R.,Tauber,R. N., Eds.; Lattice Press: Sunset Beach, California, **1987.**

2. Wantanabe, K; Tanigaki, T.; Wakayama, S., *J. Electrochem. Soc.*, **1981**, 128, 2630.

3. Rosler, R. S., *Solid State Technology*, **1977**, 20(4), 63.

4. Goldsmith, N.; Kern, W., RCA Rev., **1967**, 28, 153.

5. Cobianu, C; Pavelscu, C., *J. Electrochem. Soc.*, **1983**, 130, 1888.

6. Cobianu, C; Pavelscu, C., *Thin Solid Films*, **1984**, 117, 211.

7. Becker, F. S.; Pawlick, D.; Schafer, H.; Standigl, G., *J. Vac. Sci. Technol.*, **1986**, *B4*(3), 732

8. Huppertetz, H.; Engl, W. L., *IEEE Trans. Electron Devices*, **1979**, *ED-26,* 658

9. Hochberg, A. K.; Lagendijk, A.; O'Meara, D. L.; Klerer,J., *J. Electrochem.Soc.*, **1961**, 108, 1070.

10. Jordan , E. L., *ibid.*, **1961**, *108,* 478

11. Klereer, j., *ibid.*,**1965,** *112*(5), 503

12. Hochberg, A. K.; O'Meara, D. L., *ibid.*, **1989**, *136* (6), 1843

13. Orshonik, J.; Kraitchman, J., *ibid.*, **1968**, *115*, 649

14. Levy, R. A.; Gallagher, P. K.; Schrey, F., *ibid.*, **1987**, *134*, 430; 1744

15. Albella, J. M.; Criado, A.; Muroz Merino, E., *Thin Solid Films*, **1976**, *36*, 479

16. Levy , R. A.; Grow, J. M.; Chakravarthy, G. S., *Chem. Mater.*, **1993**, *5*, 1710

17. Huo, D. T. C.; Yan, M. F.; Foo, P. D.; *J. Vac. Sci. Technol.*, **1991**, *A9*, (5), 2602

18. Patterson, J. D.; Ozturk, M. C., *ibid.*, **1992**, *B10*(2), 625

19. Gelerrt, B., *Semicond. Int.*, **1990**, *13*, 83

20. Hochberg, A. K.; Lagendijk, A.; O'Meara, D. L.; *J. Electrochem. Soc. Ext. Abstr.*, **1988**, *88-2*, 335

21. Adams , A. C.; Capio, C.D.; *J. Electrochem. Soc.*,**1979**,*126*, 1042

22. Adams, A. C.; Alexander, F. B.; Capio, C. D.; Smith, T. E., *ibid.*, **1981**, *128*, 1545

23. Emesh, T.; D'Asti, G.; Mercier, J. S.; Leung, P., *ibid.*, **1989**, *136*, 3404

24. Fracassi, F.; D'Agostino, R.; Favia, P., *ibid.*, **1992**, *139*, 2636

25. Evert, P. G. T. Van de ven, *Solid State Technol.*, **1981**, *24*(4), 167

26. Mackens, U.; Merkt, U., *Thin Solid Films*, **1982**, *97*, 53

27. Chin, B.L.; Evert, P. G. T. Van de ven, *Solid State Technol.*, **1988**, *31*(4), 119

28. Gorthy, C. S., *Low Temperature Synthesis and Characterization of LPCVD Silicon Dioxide Films Using Diethylsilane*, MS. Thesis, Dept. of Matl. Sci. and Engg., New Jersey Institute of Technology, Newark, New Jersey, **1992**

29. Datta, A., *Synthesis of Silicon Oxide/Vycor Composite Membrane Structures by an Optimized LPCVD Process,* MS. Thesis, Dept. of Matl. Sci. and Engg., New Jersey Institute of Technology, Newark, New Jersey, **1995**.

30. *Handbook of Chemical Vapor Deposition*, 1992, P-106, Noyes Publication, Park Ridge, NJ.

31. Levy, R.A.; Grow, J., M.; and Chakravarthy, G., S.; *Chemistry of Materials*, **1993**, 5-12, 1710.

32. Brown,W.A.; Kamins,T.I., *Solid State Technol.*, **1979**, *22*(7), 51.

33. Fracassi, F., d'Agostino, R.; Favia, P., *ibid.*, **1992**,*139*(9), 2636.

34. Balija, B.,J.; Ghandhi, S., K., *J. Appl. Physics*, **1973**, 44, 990.

35. Shibata, M.; Sugawara, K.,*This Journal*, **1975**, 122, 175.

36. Kern, W.; Heim, R.,C., *ibid.*, **1960**, 116, 855.

37. Juleff, E., F., *Microelctron.*, **1975**, 6, 21

38. Chow, K.; Garrison, L., G., *ibid*, **1977**, 124, 1133.

39. Wong, J., *J. Non-Cryst. Solids*, **1968**, 29, 618.

40. Strater, K., *RCA Rev.*, **1968**, 29, 618.

41. Kern, W.; Rosler, R.,S., *J.of Vac. Sci. and Tech.*, **1977**, 14, 1082.

42. Rosler, R., S., *Solid State Tech.*, **1977**, 20(4), 1963.

43. Gorczyca, T., B; Gorowitz, B.,in *VLSI Electronics Microstructure Science*, **1984**, 8, 69.

44. Adams, A.C., in *VLSI Technology* (S.M.Sze, ed.), **1983**, p.93.

45. Adams, A.C; Capio, C.D; Haszko, S.E; Parisi, G.I; Povilonis, E.I; and McD. Robinson, *J. Electrochem. Soc.*,**1979**, 123(2), 313.

46. Adams, A.C; Murarkha, S.P, *J. Electrochem. Soc.*,**1979**, 126(2), 334.

47. Kern, W., *RCA Review*, **1976**, 37, 78.

48. Tenney, A.S.; Ghezzo,M., *J. Electrochem.Soc.*, **1973**, 120, 176.

49. Norio Tokota et al., *Journal of Lightwave Technology*, **1988**, 6(6), 1003.

50. Verbeek, B.H. et al, *Journal of Lightwave Technology*, **1988**, 6(6), 1011.